Published in final edited form as:
Dev Biol. 2015 March 1; 399(1): 139–153. doi:10.1016/j.ydbio.2014.12.026.

Sox4 regulates choroid fissure closure by limiting Hedgehog signaling during ocular morphogenesis

Wen Wen, **Lakshmi Pillai-Kastoori**, **Stephen G. Wilson**, and **Ann C. Morris***
Department of Biology, University of Kentucky, Lexington, KY 40506-0225, USA

Abstract

SoxC transcription factors play critical roles in many developmental processes, including neurogenesis, cardiac formation, and skeletal differentiation. In vitro and in vivo loss-of-function studies have suggested that SoxC genes are required for oculogenesis, however the mechanism was poorly understood. Here, we have explored the function of the SoxC factor Sox4 during zebrafish eye development. We show that *sox4a* and *sox4b* are expressed in the forebrain and periocular mesenchyme adjacent to the optic stalk during early eye development. Knockdown of *sox4* in zebrafish resulted in coloboma, a structural malformation of the eye that is a significant cause of pediatric visual impairment in humans, in which the choroid fissure fails to close. *Sox4* morphants displayed altered proximo-distal patterning of the optic vesicle, including expanded *pax2* expression in the optic stalk, as well as ectopic cell proliferation in the retina. We show that the abnormal ocular morphogenesis observed in Sox4-deficient zebrafish is caused by elevated Hedgehog (Hh) signaling, and this is due to increased expression of the Hh pathway ligand *Indian hedgehog b* (*ihhb*). Consistent with these results, coloboma in *sox4* morphants could be rescued by pharmacological treatment with the Hh inhibitor cyclopamine, or by co-knockdown of *ihhb*. Conversely, overexpression of *sox4* reduced Hh signaling and *ihhb* expression, resulting in cyclopia. Finally, we demonstrate that *sox4* and *sox11* have overlapping, but not completely redundant, functions in regulating ocular morphogenesis. Taken together, our data demonstrate that Sox4 is required to limit the extent of Hh signaling during eye development, and suggest that mutations in SoxC factors could contribute to the development of coloboma.

Keywords

Sox4; Hedgehog signaling; Indian Hedgehog; zebrafish; coloboma; eye; choroid fissure

*Corresponding author: Dr. Ann C. Morris Department of Biology University of Kentucky Lexington, KY 40506-0225 Tel: 859-257-8823 ann.morris@uky.edu.

AUTHOR CONTRIBUTIONS:
A.C.M. and W.W. conceived and designed the experiments, W.W., L.P.K., and S.G.W. performed the experiments, A.C.M., W.W., L.P.K., and S.G.W. analyzed the data, and A.C.M. and W.W. wrote the paper.

INTRODUCTION

Ocular coloboma is a developmental disorder that occurs when the choroid fissure, a transient opening that forms in the ventral portion of the optic cup, fails to properly close, causing a cleft in the inferonasal quadrant of the eye. Depending on the timing and location of the closure defect, coloboma can affect multiple regions of the developing eye, including the cornea, iris, ciliary body, retina, pigmented epithelium, and the optic nerve (Chang et al., 2006). Coloboma is often observed in conjunction with other ocular abnormalities, such as microphthalmia, anophthalmia, or anterior chamber defects, and may also be associated with more complex syndromes affecting multiple systems (Porges et al., 1992; Eccles and Schimmenti, 1999; Morrison et al., 2000; Guirgis and Lueder, 2003; Chang et al., 2006). Although coloboma represents an important cause of pediatric visual impairment, contributing to 3-11% of childhood blindness worldwide (Hornby et al., 2000), the molecular and cellular mechanisms underlying choroid fissure closure and the genetic etiology of coloboma remain poorly understood. This is partly because ocular coloboma is both phenotypically and genetically heterogeneous, and although numerous coloboma-causing genes have been identified, mutations in these genes account for only a minority of cases. Based on data from patient studies and from animal models, a coloboma gene network has been proposed, which highlights the complex relationships between several genes implicated in coloboma or associated ocular malformations (Gregory-Evans et al., 2004). The members of this network include eye field specific transcription factors (EFTFs), cell cycle regulators, and cell signaling molecules that collectively control cell proliferation, cell migration, cell fate specification, and cell death.

One of the central hubs of the coloboma gene network is the secreted molecule Sonic Hedgehog (Shh), one of the ligands for the evolutionarily conserved Hedgehog (Hh) signaling pathway. Hh signaling is critical for the correct morphogenesis, growth, and patterning of several embryonic tissues and organs, and also plays a key role in tissue regeneration, stem cell maintenance, and tumorigenesis (Ingham and McMahon, 2001; Briscoe and Therond, 2013). In the development of the visual system, Hedgehog (Hh) signaling is required at several stages. Early in development, Hh signals emanating from the ventral midline regulate the segregation of a single eye field into two bilateral optic primordia. As the optic vesicles evaginate from the forebrain, Hh signaling controls proximo-distal patterning of the optic vesicle into optic stalk and optic cup domains, respectively (Ekker et al., 1995). And after optic cup formation, Hh signaling within the developing retina regulates neurogenesis by controlling retinal progenitor cell proliferation and differentiation (Marti and Bovolenta, 2002). Reflecting its central role in oculogenesis, mutations in Shh are associated with several ocular defects, including cyclopia, microphthalmia, anophthalmia, and coloboma (Schimmenti et al., 2003; Amato et al., 2004; Gongal et al., 2011). Moreover, the downstream targets of Shh include several coloboma-causing genes (Sanyanusin et al., 1995; Slavotinek et al., 2012). However, less is known about the factors that lie upstream of Hh ligand expression – such genes may also contribute to the pathogenesis of coloboma.

We recently demonstrated that the SoxC transcription factor Sox11 is one of the upstream regulators of Hh signaling, and that in the zebrafish, Sox11 regulates choroid fissure closure

as well as retinal neurogenesis by inhibiting the expression of Shh (Pillai-Kastoori et al., 2014). The Sox proteins are named for a shared motif called the SRY box, a high-mobility-group (HMG) DNA binding domain homologous to the DNA-binding domain of the mammalian sex-determining gene SRY. Based on amino acid identity within the HMG domain, Sox proteins are divided into 8 groups (A to H). The SoxC group includes Sox4, Sox11 and Sox12 (Bowles et al., 2000). SoxC family members display overlapping expression domains in several embryonic tissues, including neuronal and mesenchymal progenitor cells (Dy et al., 2008). The SoxC factors function redundantly in the development of some tissues, such as the nervous system, but also have distinct roles in the development of other tissues, such as the heart (Bergsland et al., 2006; Bhattaram et al., 2010; Penzo-Mendez, 2010; Paul et al., 2013). Moreover, Sox11 null mice survive several days longer than Sox4 null mice, suggesting non-redundant roles for these two proteins in early embryogenesis.

In this study, we examined the function of Sox4 in zebrafish ocular development. Like Sox11, Sox4 is expressed in multiple embryonic tissues, including the retina (Dy et al., 2008; Usui et al., 2013; Pillai-Kastoori et al., 2014). In the mouse, Sox4 expression initiates in the central retina near the optic nerve at E11.5. As retinal development proceeds, Sox4 is expressed in the ganglion cell layer (GCL) and the neuroblastic layer (NBL). Constitutive *Sox4* null mice die at E14.5 due to severe cardiac malformation and defects in B lymphocyte differentiation (Schilham et al., 1996), precluding a more thorough assessment of Sox4's role in ocular development in this model. A conditional *Sox4* knockout mouse in which *Sox4* is deleted in the developing retina displayed a modest reduction in ganglion cell number, but no other ocular defects were reported, and the effect of *Sox4* deletion on Hh signaling was not investigated (Jiang et al., 2013).

Zebrafish possess two co-orthologs of the mammalian *Sox4* gene: *sox4a* and *sox4b*. Previously, microarray analysis of retinal mRNA from a zebrafish model of chronic rod photoreceptor degeneration and regeneration revealed that *sox4a* and *sox4b* mRNA levels are up-regulated in response to rod photoreceptor loss (Morris et al., 2011), suggesting they function in rod regeneration. However, the role of *sox4a/b* in embryonic zebrafish ocular development was not known. In this study, we show that Sox4 is required for choroid fissure closure and proper proximo-distal patterning of the optic vesicle in zebrafish. We also demonstrate that loss of Sox4 affects retinal progenitor cell proliferation. Furthermore, we show that similar to loss of Sox11, the ocular phenotypes of Sox4-deficient zebrafish are caused by elevated Hh signaling. However, in contrast to Sox11, we found that Sox4 primarily regulates expression of the Hh signaling ligand Indian Hedgehog (Ihh), rather than Shh. Therefore, our data demonstrate that Sox4 and Sox11 together control levels of Hh signaling during ocular development by regulating expression of distinct Hh ligands, and suggest that SoxC factors may be additional members of the coloboma gene network.

RESULTS

Sox4a and sox4b are expressed in periocular tissues and the developing retina

We performed fluorescent in situ hybridization (FISH) with antisense probes for *sox4a* and *sox4b* to determine their expression patterns in the forebrain and the eye during zebrafish

embryonic development. Previous studies reported expression of *sox4* as early as the 5 somite stage (approximately 12 hours post fertilization, hpf) in the lateral plate mesoderm and mid-trunk endoderm of zebrafish embryos, respectively (Mavropoulos et al., 2005). Using FISH, we detected *sox4a* expression in the dorsal forebrain and around the optic stalk at 12 hpf, (Figure 1A-A"). *Sox4b* was not detectable at this time point. At 18 hpf, during optic vesicle invagination to form the bi-layered optic cup, expression of *sox4a* was detected in cells on either side of and directly adjacent to the optic stalk (Figure 1B). More posteriorly, *sox4a* expression was observed in periocular cells in the dorsal diencephalon (Figure 1B'-B"). Expression of *sox4b* was also occasionally observed in this region, although not in all embryos analyzed (Figure 1C'-C"). Some of the *sox4a*-positive periocular cells were of neural crest origin, as they co-localized with GFP+ cells in the *sox10:EGFP* transgenic line (Hoffman et al., 2007) (Figure 1F, arrows). At 24 hpf, expression of both *sox4* paralogs was observed in the ventral diencephalon adjacent to the retina (Figure 1D-E"), and *sox4a* expression persisted in the dorsal *sox10:EGFP*+ periocular mesenchyme (Figure 1H). Expression of *sox4a* and *sox4b* was first observed in the ventronasal retina at 36 hpf (Figure 1J-K), coinciding with the onset of retinal neurogenesis. These *sox4*+ cells did not co-localize with PCNA, a marker for proliferating cells, suggesting that they were postmitotic (Figure 1P-U). At 48 hpf, *sox4a* expression was detected in the inner half of the inner nuclear layer (INL), whereas *sox4b* was expressed in both the ganglion cell layer (GCL) and the inner portion of the INL (Figure 1L-M). Some of the *sox4a/b*-positive cells co-localized with the ganglion and amacrine cell marker HuC/D at 48 hpf (Figure 1W-X"). At 72 hpf, scattered expression of *sox4a* and *sox4b* was observed in the outer half of the INL, and expression of *sox4a/b* was also detected in the ciliary marginal zone (CMZ), the persistently neurogenic region at the periphery of retina (Figure 1N-O). The *sox4a/b*-positive cells in the CMZ were located in the central CMZ and mostly did not co-localize with PCNA (Figure 1T-U), suggesting that *sox4a/b* marks postmitotic neuronal precursors in this region. In the distal INL, rare *sox4b*-positive cells co-localized with the horizontal cell marker Prox1, however the *sox4a*-positive cells did not co-localize with horizontal, bipolar, or Müller cell markers (Figure S1). Instead, we found that some *sox4a*-positive cells in the outer INL also expressed *crx* (Figure 1Y-Y"), suggesting that *sox4a* may be expressed in some photoreceptor progenitors (Nelson et al., 2008). Taken together, the early expression of *sox4* adjacent to the optic stalk and evaginating optic vesicle, and later expression within the developing retina, suggests that it functions during zebrafish ocular development.

Knockdown of sox4 causes ocular coloboma

Translation blocking morpholinos (MOs) targeting the 5'-UTR upstream of the translation start site were used to knock down *sox4a/b* expression in zebrafish embryos. The efficiency of each *sox4* MO was assessed by co-injecting an EF1α-EGFP plasmid containing the MO binding site. At 24 hpf, 91.94± 1.93% of the control MO injected embryos displayed GFP expression; in contrast, none of the *sox4* MO injected embryos showed any GFP expression, indicating that the *sox4* MOs are highly efficient in blocking target gene translation (Figure S2A-E). Morpholino-injected embryos were scored for ocular phenotypes at 24, 48, and 72 hpf by light microscopy. Since some toxicity was observed in *sox4* morphants, a p53 MO was co-injected to inhibit non-specific cell death. Knockdown of *sox4a* resulted in ocular

coloboma in 12.23± 2.89% of embryos (n= 17/139), whereas knockdown of *sox4b* caused coloboma in 9.24±2.79% of embryos (n= 11/119). Knockdown of both *sox4a/b* simultaneously caused coloboma in 47.84 ± 7.32% of embryos (n= 133/278), suggesting a synergistic effect on the phenotype (Figure S2F). In all subsequent experiments, *sox4a* and *sox4b* MOs were co-injected, and *sox4a/b* MO-injected embryos are referred to as *sox4* morphants. Occasionally, pericardial edema and a curved tail were also observed in *sox4* morphant embryos (data not shown). However, as these phenotypes can be produced by non-specific activity of MOs, we did not analyze them further. We observed a higher incidence of coloboma (76.92%, n= 130/169) in *sox4* morphants without the p53 MO, suggesting that cell death may also contribute to the coloboma phenotype (data not shown).

We performed three separate experiments to confirm the specificity of the *sox4* morphant coloboma phenotype. First, a second set of non-overlapping *sox4* MOs was used, which produced a similar proportion of choroid fissure closure defects to the first set (Figure S2G-J). Second, *sox4a* and *sox4b* mRNAs (lacking the MO binding site) were co-injected with the *sox4* MOs, and the embryos were scored for coloboma at 48 hpf. Co-injection of *sox4a/b* mRNA significantly reduced the incidence of coloboma in *sox4* morphants to 16.49% ± 3.37% (Fisher's exact test, P<0.0001; Figure 2A"-D", 2G), suggesting that this phenotype resulted from specific knockdown of *sox4*. Finally, we utilized the CRISPR/Cas9 system (Hruscha et al., 2013; Hwang et al., 2013; Jao et al., 2013; Talbot and Amacher, 2014) to target mutations to the *sox4a* and *sox4b* genomic loci. For each gene, single guide RNAs (sgRNAs) were designed to target two different sites within the coding region, neither of which overlapped with the MO target sequence. In founders injected with Cas9 mRNA and *sox4a* or *sox4b* sgRNAs, we observed coloboma in 31.19± 6.40% (n= 13/44) and 20.91± 8.14% (n= 9/48) of injected embryos, respectively (Figure S1M-O). In contrast, none (n= 0/201) of the uninjected controls (UIC) displayed coloboma, and only 1.33± 2.31% (n= 1/89) of embryos injected with a *tyrosinase* (*tyr*) sgRNA/Cas9 exhibited coloboma, although *tyr* sgRNA/Cas9 was very effective at inducing pigmentation defects, as previously described (Jao et al., 2013) (Figure S1K-L, S1O). High resolution melt curve analysis (HRMA) and sequencing of the *sox4a* and *sox4b* target regions in individual injected embryos confirmed that short indels were generated in the *sox4* gRNA/Cas9 injected individuals with high efficiency (Figure S1P-Q and data not shown), with the mutation frequency ranging from 52.78% to 94.44%. These data suggest that the CRISPRs induced bi-allelic gene inactivation in mosaic injected embryos, as has been reported previously in zebrafish and mice (Jao et al., 2013; Yen et al., 2014; Zhang et al., 2014), resulting in ocular phenotypes similar to those seen in the *sox4* morphants. Taken together, these results strongly support the specificity of the *sox4* morphant coloboma phenotype.

The first sign of an ocular defect in *sox4* morphants was detected at the 8-10 somite stage (12-14 hpf), when the horizontal crease (formed during the evagination of the optic vesicle), becomes visible. Compared to the control morphants, the *sox4* morphants that developed ocular coloboma at 48 hpf always displayed a "crooked" horizontal crease at 12-14 hpf (Figure 2A', arrow), suggesting that the coloboma resulted from an earlier ocular morphogenesis defect. At 24 hpf, the two lips on either side of the choroid fissure in the ventral retina were either wide open or bent backwards in *sox4* morphants (Figure 2B'). The

persistently open choroid fissure was more obvious at 48 and 72 hpf, because this region of the ventral retina appeared to lack pigmentation of the underlying retinal pigmented epithelium (RPE) (Figure 2C'). Ventral views of *sox4* morphant embryos revealed a hole in the posterior RPE through which the retinal tissue extruded into the brain, which accounts for the apparent lack of pigmentation in this region when viewed laterally (Figure 2D'). Histological sections of 72 hpf control and *sox4* morphant embryos clearly demonstrated the extrusion of colobomatous tissue through the open choroid fissure (Figure 2F, asterisk). Sox4-deficient retinas also displayed less mature lamination compared to control retinas, however all three retinal cell layers were present.

We immunolabeled control and *sox4* morphant embryos with an antibody that recognizes laminin, which is present in the basement membrane surrounding the optic cup. As the nasal and temporal lips of the retina on either side of the choroid fissure fuse together, laminin is degraded and disappears. In control morphants at 48 hpf, laminin immunostaining revealed that the nasal and temporal lobes of the choroid fissure were closely apposed, but not yet fused (Figure 3A-A'). In contrast, the choroid fissure was much wider in *sox4* morphants at this time (Figure 3B-B'). By 72 hpf in control morphants, only faint expression of a single layer of laminin was visible at the now closed choroid fissure; however, in *sox4* morphants the choroid fissure remained open with two distinct layers of laminin outlining the unfused lips of the nasal and temporal retina (Figure 3C-D').

Proximo-distal patterning of the optic vesicle is altered in Sox4-deficient zebrafish

Coloboma can result from an abnormal or enlarged optic stalk, which may arise when there is a shift in the cell fate boundary between the optic stalk and the optic vesicle (Chang et al., 2006). We performed FISH on control and *sox4* morphant sections to examine the expression of *pax2a* and *pax6a*, which mark the optic stalk and optic vesicle domains, respectively. In control morphants at 18 hpf, *pax2a* expression was restricted to a wedge of cells located between the optic vesicle and the brain, and *pax6a* expression was evident throughout the optic vesicle (Figure 3E). In *sox4* morphants however, the region of *pax2a* expression was expanded into the optic vesicle, and there was a corresponding retraction of *pax6a* expression (Figure 3F). The expansion of *pax2a* expression in *sox4* morphants persisted at 48 and 72 hpf, where it was particularly prominent in the ventral retina around the open choroid fissure (Figure 3G-H and data not shown). The changes in *pax2a* and *pax6a* expression in *sox4* morphants were confirmed by quantitative RT-PCR (qPCR), which showed that in *sox4* morphant heads at 18 hpf *pax2a* was significantly up-regulated (1.69±0.25 fold) while *pax6a* was significantly down-regulated (2.0±0.08 fold; Figure 3I). This result indicates that the proximo-distal patterning of the optic vesicle was disrupted in Sox4-deficient embryos.

Sox4-deficient retinas display ectopic cell proliferation

Altered retinal progenitor cell proliferation has been observed in coloboma models (Kim et al., 2007; Liu et al., 2012). We used an antibody to phosphohistone H3 (PH3) to label mitotic cells in control and *sox4* morphant eyes. At 18 and 24 hpf, no apparent difference was observed between control and *sox4* morphants (Figure 4A-E). At 36 and 48 hpf, the total number of PH3+ cells in the retina was significantly reduced in *sox4* morphants

compared to controls. Interestingly, some PH3+ cells were ectopically located in the inner retina of *sox4* morphants, whereas in controls PH3+ cells were all aligned at the apical border of the retina (Figure 4A, 4F-I). At 72 hpf, when retinal differentiation is largely complete, PH3+ cells in control morphant retinas were confined to the peripheral CMZ (Figure 4J). *Sox4* morphant retinas possessed PH3+ cells at the CMZ as well, but we also observed ectopic PH3+ cells in the GCL, which clustered with PCNA-positive cells (Figure 4K). These cells did not express the retinal ganglion cell marker Zn8, or the retinal progenitor cell gene *pax6a* (Figure S3). We also observed PCNA-positive cells within the colobomatous tissue protruding from the *sox4* morphant retinas (Figure 4K). Taken together, these data suggest that overproliferation does not contribute to the coloboma phenotype of *sox4* morphants, since no difference in cell proliferation was observed at 18 or 24 hpf, by which time abnormal ocular morphogenesis was evident. However, *sox4* does appear to influence cell proliferation in the retina, as knockdown caused an overall reduction in the number of dividing cells as well as ectopic cell proliferation in the GCL.

We performed a TUNEL assay to determine whether apoptosis was elevated in *sox4* morphant retinas. No apparent difference was observed at 18, 24, and 72 hpf in the number of TUNEL-positive cells in the optic vesicle/retina between control and *sox4* morphant eyes (Figure 4L). However, at 18 hpf the number of TUNEL-positive cells was significantly higher in the optic stalk region of *sox4* morphants compared to controls (Figure 4N, arrows; Fig. 4W, Student's *t*-test, $P < 0.05$). Also, at 48 hpf *sox4* morphant retinas possessed a highly variable, but significantly greater number of TUNEL-positive cells than control retinas (Figure 4L, 4S-T). Moreover, as mentioned previously we observed an increased proportion of embryos with coloboma when the p53 MO was omitted from the injection (data not shown). Taken together, these data suggest that apoptosis, particularly within the optic stalk region may contribute to the severity of the coloboma phenotype.

Hh signaling is elevated in Sox4-deficient zebrafish

As mentioned previously, we have shown that knockdown of Sox11 causes coloboma due to an elevation of Hh signaling (Pillai-Kastoori et al., 2014). Moreover, the coloboma phenotype in both *sox11* and *sox4* morphants resembles other animal models of overactive Hh signaling (Lee et al., 2008; Bassett et al., 2010; Lee et al., 2012; Zhang et al., 2013). Therefore, we asked whether cyclopamine, a pharmacological Hh inhibitor, could reduce the incidence of coloboma in *sox4* morphants. We treated *sox4* morphants with 2 μM cyclopamine, a concentration which did not produce any ocular defects on its own (Figure 5E), and which was shown previously to rescue the coloboma phenotype in zebrafish *blowout* mutants (which carry a mutation in the *ptch2* receptor) and *sox11* morphants (Lee et al., 2008; Pillai-Kastoori et al., 2014). *Sox4* morphants were exposed to either cyclopamine or an equivalent amount of ethanol vehicle from 5.5 to 13 hpf, and then analyzed at 48 hpf for the presence of coloboma. In vehicle-treated *sox4* morphants, 57.78±2.28% of embryos (n= 104/180) displayed coloboma at 48 hpf, consistent with our previous results. In contrast, cyclopamine treatment suppressed the incidence of coloboma to 15.87±2.20% (n= 26/165; Fisher's exact test, $P<0.0001$; Figure 5A-E). Treatment of *sox4* morphants with cyclopamine from 10 to 24 hpf also significantly decreased the proportion of embryos with coloboma, however the effect was not as strong as with the earlier treatment period (data not shown).

To confirm that Hh signaling was elevated in response to *sox4* knockdown, we injected *sox4* MOs into heterozygous *ptch2:EGFP* transgenic embryos, which report on Hh signaling by expressing GFP in cells that activate the Hh target gene *ptch2* (Shen et al., 2013). Elevation of GFP in the ventral forebrain was observed in *sox4* morphants as early as 12 hpf and through 72 hpf in *sox4* morphants (Figure 5F-I and data not shown), confirming that Hh signaling was indeed upregulated in Sox4-deficient embryos. To quantify the elevation of endogenous *ptch2* expression in *sox4* morphants, we performed qPCR on mRNA from control and *sox4* morphant embryos at 8, 10, and 12 hpf. We found that *ptch2* was upregulated in *sox4* morphants by more than 2-fold at all time points (Figure 5J). Taken together, these data indicate that knockdown of Sox4 results in an elevation in Hh signaling in the early embryo that leads to ocular morphogenesis defects and coloboma.

Sox4 negatively regulates expression of Indian hedgehog b (ihhb)

In Sox11-deficient zebrafish, elevation of Hh signaling is caused by an increase in expression of the Shh gene [*shha*; (Pillai-Kastoori et al., 2014)]. To determine whether Sox4 also regulates expression of *shha* or some other component of the Hh signaling pathway, we performed qPCR on mRNA prepared from the control and *sox4* morphant embryos at 8, 10, and 12 hpf, and from the heads of control and *sox4* morphant embryos at 18 and 24 hpf. Intriguingly, we found that expression of *shha* was not significantly different in *sox4* morphants compared to controls at any time point. However, expression of the Hh ligand *ihhb* was significantly upregulated in *sox4* morphants as early as 8 hpf and was strongly upregulated at 18 and 24 hpf (Figure 6A, Figure S4, Student's *t*-test, $P<0.01$). We also detected a more variable increase in expression of *ptch1*, *ptch2*, and *gli1* in *sox4* morphants at 18 and 24 hpf (Figure S4). We confirmed the upregulation of *ihhb* transcript in *sox4* morphants at 12 and 24 hpf by whole mount in situ hybridization (WISH), which revealed that *ihhb* expression in *sox4* morphants was upregulated in the ventral midline at 12 hpf (Figure 6C), and at 24 hpf *ihhb* expression was upregulated in the hypothalamus and ventral diencephalon, and had also expanded into regions of the telencephalon and dorsal diencephalon that did not express *ihhb* in controls (Figure 6E). However, the increase in *ihhb* expression in *sox4* morphants was not ubiquitous, as *ihhb* expression in the posterior notochord was similar to controls at 24 hpf (Figure 6G). We also confirmed that Ihhb protein levels were elevated in 24 hpf *sox4* morphant heads by Western blot (Figure 6H). Moreover, qPCR of mRNA prepared from cyclopamine-treated *sox4* morphants revealed that expression of *ihhb* returned to control levels following cyclopamine treatment (Figure 6I). Taken together, these results demonstrate that knockdown of Sox4 causes an increase in Hh signaling primarily through upregulation of *ihhb* expression.

Next, we co-injected an *ihhb* MO together with the *sox4* MOs and quantified the incidence of coloboma at 48 hpf. Co-injection of the *ihhb* MO significantly reduced the incidence of coloboma in *sox4* morphants in a dosage dependent manner: 19.33± 2.52% (n= 14/75) of *sox4* morphant embryos displayed coloboma when 0.5 ng of *ihhb* MO was injected (compared to 51.24± 2.70% with *sox4* MO alone), whereas injecting 1.0 ng of *ihhb* MO suppressed coloboma to 10.67± 2.08% (n= 9/91; Figure 6J). We also co-injected a previously described *shha* MO (Nasevicius and Ekker, 2000) with the *sox4* MOs to determine whether it could rescue the coloboma phenotype. When 2.0 ng of *shha* MO was

injected the proportion of embryos with coloboma was not significantly different from that observed with *sox4* MO alone (Figure 6J). However, 3.0 ng of *shha* MO did significantly reduce coloboma to 34.39 ± 5.03% (n= 79/229; Fisher's exact test, P=0.0001), although the extent of rescue was not as strong as with the *ihhb* MO. Together, these results confirm that Sox4 negatively regulates the expression of *ihhb* and that elevated *ihhb* expression in Sox4-deficient zebrafish causes coloboma.

Since knockdown of Sox4 caused an elevation in *ihhb* expression and Hh signaling, we predicted that overexpression of Sox4 would result in a corresponding reduction in Hh activity. We injected in-vitro synthesized control or *sox4a/b* mRNA into wild type embryos, and scored the injected embryos at 24 hpf for the presence of cyclopia, a phenotype associated with reduced Hh activity from the midline (Ekker et al., 1995). Whereas only 0.78±1.34 % of embryos (n= 1/128) injected with a control *Td-Tomato* mRNA exhibited cyclopia, we detected cyclopia in 36.54 ± 5.10% (n= 38/104) of the *sox4* mRNA-injected embryos (Figure 7A-B). In addition, we found that the cyclopic embryos often possessed a truncated body and U-shaped somites (Figure 7C-F), a phenotype that is also observed with reductions in Hh signaling (Currie and Ingham, 1996; Schauerte et al., 1998; Wolff et al., 2003). To confirm that the cyclopic phenotype was specific for overexpression of *sox4*, we injected the same total amount of mRNA containing different ratios of control *Td-Tomato* and *sox4* mRNA. We observed that both the occurrence and severity of cyclopia increased with increasing concentration of *sox4* mRNA (Figure 7G), strongly suggesting that the cyclopic phenotype was not an artifact of mRNA injection. qPCR performed on mRNA prepared from the heads of injected embryos confirmed that *ihhb* expression was reduced in the embryos overexpressing *sox4* at 18 and 24 hpf, although the reduction was not statistically significant at 24 hpf (Figure 7H; Student's *t*-test, P= 0.0565). Surprisingly, although *sox4* knockdown did not affect the expression level of *shha*, *sox4* overexpression significantly reduced the expression of *shha* in the head. Taken together, these data suggest that *sox4* can negatively regulate the expression of both *ihhb* and *shha*, and that overexpression of *sox4* causes a reduction in midline Hh activity, leading to cyclopia.

Bmp7 is a potential intermediate between sox4 and ihhb

Our results support the hypothesis that Sox4 is a negative regulator of *ihhb* expression. However, SoxC transcription factors are known to act as transcriptional activators rather than repressors (van de Wetering et al., 1993; Bergsland et al., 2006). Therefore, we hypothesized that Sox4 indirectly inhibits *ihhb* expression by activating an intermediate repressor. One candidate Hh repressor is Bmp7. Bmp7 is known to modulate Hh signaling (both positively and negatively), was previously shown to be significantly down-regulated in Sox11-deficient zebrafish and *Sox11* null mice, and *bmp7* mRNA can partially rescue coloboma in *sox11* morphants (Pathi et al., 1999; Seki and Hata, 2004; Manning et al., 2006; Bastida et al., 2009; Duench and Franz-Odendaal, 2012; Pillai-Kastoori et al., 2014). Moreover, *Bmp7* mutant mice display ocular malformations such as microphthalmia and optic fissure defects (Morcillo et al., 2006). We performed qPCR for *bmp7b* transcript levels in controls and *sox4* morphants at 8, 10, 12, 18 and 24 hpf. This analysis revealed that *bmp7b* expression was significantly downregulated at all time points in *sox4* morphants (Figure 8A, Student's *t*-test, P< 0.01). We then injected *bmp7b* mRNA along with the *sox4*

MO and found that this partially rescued the coloboma phenotype of *sox4* morphants (Figure 8B, Student's *t*-test, P< 0.01). These data suggest that Sox4 may negatively regulate Ihhb at least in part through the activation of Bmp7b. We also analyzed the expression of four additional regulators of Hh signaling: two Hh inhibitors (*fgfr2* and *kras*), and two Hh activators (*lhx8* and *nkx6.1*; (Cai et al., 2000; Flandin et al., 2011; Mukhopadhyay et al., 2013). *Fgfr2* was downregulated in *sox4* morphant heads at 18 hpf and *lhx8* was upregulated in *sox4* morphants at 12 hpf, suggesting that these genes may also function downstream of Sox4 and upstream of Hh signaling during eye development (Figure S5, Student's *t*-test, P<0.05).

Sox4 and sox11 have overlapping functions in regulating choroid fissure closure

Our previous work demonstrated that Sox11-deficient zebrafish, similar to *sox4* morphants, exhibit ocular coloboma and elevated Hh signaling. Moreover, *sox4* mRNA injection can significantly reduce the incidence of coloboma in *sox11* morphants (Pillai-Kastoori et al., 2014). To further investigate the functional overlap between Sox4 and Sox11, we injected *sox4* and *sox11* MOs, either alone or together, at half the usual dose. When a half-dose of *sox4* MO was injected, only 11.05± 3.15% (n= 16/145) of morphants exhibited coloboma at 48 hpf. Similarly, when a half-dose of *sox11* MO was injected, 22.31± 4.00% (n= 16/71) of the morphants exhibited coloboma. However, co-injection of half-doses of *sox4* and *sox11* MOs together resulted in 72.47± 2.95% (n= 51/70) of embryos with coloboma (Figure 9A-H, 9I), suggesting that knockdown of the two SoxC factors simultaneously produced a synergistic effect on the coloboma phenotype. Furthermore, injection of *sox11a/b* mRNA into *sox4* morphants significantly suppressed the incidence of coloboma from 41.09±7.36% (n= 113/275) to 10.14± 3.09% (n= 28/276, Figure 9J). We did not detect abnormalities in lens development in *sox4* morphants (Figure 9C, arrow). Moreover, the proportion of embryos with a malformed lens was not increased by addition of the *sox4* MO (data not shown). Taken together, these results indicate that Sox4 and Sox11 have partially overlapping roles in regulating choroid fissure closure and can functionally compensate for one another during ocular morphogenesis, but are not functionally redundant with respect to lens development.

DISCUSSION

Although many genes have been identified that contribute to coloboma (Chang et al., 2006), the molecular mechanisms of choroid fissure closure have not been completely elucidated. It has been shown in animal models as well as in human patients that alterations in Hh signaling can cause coloboma (Schimmenti et al., 2003; Take-uchi, 2003; Lee et al., 2008; Lee et al., 2012). However, not much is known about how proper levels of Hh activity are maintained during eye development. In this study, we demonstrated that successful choroid fissure closure requires the activity of Sox4 to limit both the level and extent of expression of the Hh pathway ligand Ihh, permitting proper proximo-distal patterning of the optic stalk and vesicle. Together with our previous work demonstrating a role for Sox11 in controlling expression of Shh during ocular development (Pillai-Kastoori et al., 2014), our studies firmly place the SoxC transcription factors upstream of the Hh signaling pathway in the complex genetic network that regulates vertebrate choroid fissure closure.

The involvement of both Sox4 and Ihh in choroid fissure closure is a novel result, but is consistent with previous work demonstrating that related family members (Sox11 and Shh, respectively) also participate in this process. Although coloboma was not reported in the Sox4 null mutant mouse (Schilham et al., 1996; Cheung et al., 2000), the early lethality of that model likely precluded a thorough characterization of any ocular phenotypes. Coloboma was also not reported in a conditional mouse mutant lacking Sox4 expression within the developing eye (Jiang et al., 2013). However, our cyclopamine rescue data suggest that the coloboma phenotype of *sox4* morphants is caused by disruption in early, midline-derived Hh signaling, likely due to loss of *sox4* expression in the forebrain and/or periocular mesenchyme (POM). Therefore, alterations to *Sox4* expression within the optic vesicle may not have been sufficient to cause coloboma. Finally, 65% of patients with CHARGE syndrome, a genetic disorder characterized by coloboma and cardiac abnormalities in addition to other birth defects, carry a mutation in *CDH7* (Chang et al., 2006), which directly activates *Sox4* and *Sox11* (Feng et al., 2013). Therefore, it is possible that altered expression of Sox4 (and/or Sox11) underlies the coloboma phenotype observed in CHARGE syndrome patients.

Our data strongly suggest that knockdown of Sox4 results in an early elevation of midline-derived Hh signaling, which ultimately results in defects in ocular morphogenesis and coloboma. How might this occur? We observed that the expression of the optic stalk marker *pax2a* was significantly expanded into the optic vesicle of *sox4* morphants. As Hh signaling has a well-established role in specifying the optic stalk region through regulation of Pax2 expression, our results suggest that the elevation in Hh signaling from the midline expands the region of the optic vesicle that is fated to become optic stalk tissue. The decrease in *bmp7b* expression in *sox4* morphants may also contribute to the defect in proximo-distal patterning of the optic stalk and vesicle, as others have shown previously that Bmp7 is required prior to Hh signaling for proper expression of Pax2 in the optic disk (Morcillo et al., 2006). In conjunction with (or as a result of) reduced Bmp7 and expanded Pax2, we observed an increase in apoptosis in the optic stalk region at 18 hpf. Therefore, we propose that misspecification of the optic vesicle cells as optic stalk physically interferes with proper closure of the choroid fissure, resulting in coloboma, and that the abnormally specified optic stalk cells ultimately die by apoptosis.

Although many studies in animal models and humans have demonstrated the critical role of Shh in the morphogenesis and patterning of the developing eye (Amato et al., 2004), there are much less data on the role of Ihh, which is better known for its function in regulating skeletal and intestinal development (St-Jacques et al., 1999; Seki and Hata, 2004; Kosinski et al., 2010). However, some previous studies are consistent with our finding that Ihh levels influence ocular development. For example, overexpression of murine Ihh in zebrafish embryos caused expansion of *pax2* expression in the optic stalk (Hammerschmidt et al., 1996), and in the mouse, Ihh was shown to be required for proper development of the RPE and peri-ocular tissues (Dakubo et al., 2008). Interestingly, although we observed a significant elevation (approximately 4-fold) of *ihhb* expression at 8-12 hpf in *sox4* morphants, this increase was even more pronounced at 18 and 24 hpf (approximately 15-fold). This suggests that *ihhb* is itself a target of Hh signaling, resulting in a feedback loop of

enhanced expression when Hh signaling is increased. A similar feedback loop with respect to Hh signaling and *shha* expression has been observed previously (Pillai-Kastoori et al., 2014), suggesting that this may be a general phenomenon of Hh signaling and Hh ligand expression.

Similar to other studies of SoxC family members, our results indicate that Sox4 and Sox11 have overlapping, but not completely redundant, functions in eye development. Thus, although *sox4* and *sox11* were able to compensate for each other when ectopically overexpressed, we observed distinct differences in their knockdown phenotypes. First, although knockdown of either *sox11* or *sox4* resulted in coloboma, abnormal lens development was only observed following knockdown of *sox11*. Second, the penetrance of the coloboma phenotype was higher in Sox11-deficient zebrafish than in Sox4-deficient zebrafish [~70% versus ~50%, respectively; this study and (Pillai-Kastoori et al., 2014)]. And third, whereas both *sox11* and *sox4* morphants displayed elevated Hh signaling, this occurred through increased expression of distinct Hh ligands (*shha* and *ihhb*, respectively).

These phenotypic differences may be explained by the differing expression patterns of *sox11* and *sox4*. For example, whereas both *sox4* and *sox11* are expressed in the diencephalon adjacent to the optic vesicle at 18 and 24 hpf, *sox4* (but not *sox11*) is also expressed in the periocular mesenchyme (POM). As the POM was previously shown to be a target of Ihh but not Shh signals in the mouse eye (Dakubo et al., 2008), *sox4* expression in the POM may function in a negative feedback mechanism to limit the level or duration of Ihh signaling there. Similarly, *sox11*, (but not *sox4*) is expressed in the developing zebrafish lens, which may account for the unique lens phenotype in *sox11* morphants. Finally, the differing penetrance of the coloboma phenotype between the two knockdown models may be due to differences in their transactivation properties, as previous work has shown that Sox11 is a stronger transcriptional activator than Sox4 (Dy et al., 2008).

Targeted disruption of Sox4 or Sox11 in the developing mouse retina results in a reduction in retinal ganglion cell (RGC) number and optic nerve thickness (Jiang et al., 2013). Although we detected expression of both *sox4* and *sox11* in the zebrafish GCL during retinal development, we did not observe a loss of ganglion cells in either *sox4* or *sox11* morphants (data not shown). It is possible that we failed to detect an early delay in RGC differentiation due to the much shorter window of retinal neurogenesis in the zebrafish compared with mouse (Cepko et al., 1996; Stenkamp, 2007). Alternatively, it is possible that knockdown of both *sox4* and *sox11* is required to alter RGC formation in the zebrafish.

Although we did not detect a loss of RGCs, we did observe ectopic cell proliferation in the GCL of the *sox4* morphant retina. This phenotype has been observed in other models of overactive Hh signaling, such as zebrafish and mouse Ptch receptor mutants (Moshiri and Reh, 2004; Bibliowicz and Gross, 2011), and is consistent with the known role of the Hh pathway in promoting retinal progenitor cell proliferation. However, we also found that the total number of proliferating cells was reduced in the retinas of *sox4* morphants at 36 and 48 hpf, whereas it was elevated at 72 hpf. These seemingly contradictory results could be explained by alterations in the cell cycle kinetics of RPCs, either via elevated Hh signaling [as described by (Locker et al., 2006)] or through a Hh-independent role of Sox4 in

regulating cell cycle exit. Alternatively, the ectopically located proliferating cells in *sox4* morphant retinas could indicate disruptions in the organization of the retinal neuroepithelial cells. Finally, it is not clear whether the altered cell proliferation in the retina is due to loss of *sox4* expression (and the subsequent elevation in Hh signaling) from the midline, or from within the retina itself. Future studies may be able to separate the early and later functions of Sox4 in eye development using photo-morpholinos or inducible transgenes to control the timing of *sox4* inactivation and rescue.

MATERIALS AND METHODS

Zebrafish strains and maintenance

All zebrafish (*Danio rerio*) strains were bred, raised, and maintained at 28.5° C on a 14 hour light:10 hour dark cycle according to established protocols (Westerfield, 2000). The *Tg(gfap:GFP)mi2001* transgenic line (Bernardos et al., 2007), hereafter called *gfap*:*GFP*, was obtained from the Zebrafish International Resource Center (ZIRC, Eugene, OR). The *Tg(GBS-ptch2:nlsEGFP)* transgenic line (Shen et al., 2013), hereafter called *ptch2:EGFP*, was kindly provided by R. Karlstrom (University of Massachusetts, Amherst, MA). The *Tg(−7.2sox10:EGFP)*^{zf77} transgenic line (Hoffman et al., 2007), hereafter called *sox10:EGFP*, was generously provided by B.A. Link (Medical College of Wisconsin, Milwaukee, WI). Embryos were staged according to established developmental hallmarks (Kimmel et al., 1995). All animal procedures were carried out in accordance with guidelines established by the University of Kentucky Institutional Animal Care and Use Committee.

Whole mount in situ hybridization (WISH) and fluorescent in situ hybridization (FISH)

Antisense RNA probes were prepared by in vitro transcription of linearized plasmids containing a portion of the coding sequence of the gene of interest, using SP6, T7, or T3 polymerase and digoxigenin (DIG) or fluorescein (FITC) labeling mix (Roche Applied Science, Indianapolis, IN). The *sox4a* plasmid was prepared by cloning PCR products into the pGEM-T-easy vector (Promega, Madison, WI). The sequences of all PCR primers used in this study are given in Table S1. The *sox4b* plasmid (Mavropoulos et al., 2005) was generously provided by Bernard Peers (Université de Liège, Sart Tilman, Belgium). The *ihhb* plasmid (Chung et al., 2013) was generously provided by H.C. Park (Korea University, Ansan, Gyeonggido, Republic of Korea). The *crx* and *pax6a* plasmids (Shen and Raymond, 2004; Ochocinska and Hitchcock, 2007) were kindly provided by Y.F. Leung (Purdue University, West Lafayette, IN). The *pax2a* plasmid (Lee et al., 2008) was kindly provided by J.M. Gross (University of Texas, Austin, TX). WISH and FISH were performed as previously described (Forbes-Osborne et al., 2013; Pillai-Kastoori et al., 2014). Images were obtained on an inverted fluorescent microscope (Eclipse Ti-U; Nikon Instruments).

Morpholino and mRNA microinjection

All morpholinos (MOs) were obtained from Gene Tools, LLC (Philomath, OR) and injected into zebrafish embryos at the one- to two-cell stage. The following MOs were used in this study: standard control MO: 5’-CCTCTTACCTCAGTTACAATTTATA-3’; *sox4a* MO1: 5’-GCGCTAAGAGTCTTTCTTCTTCACT-3’; *sox4b* MO1: 5’-ACGCGCCTTCAGTCGTGCTTAGTGC-3’; *ihhb* MO: 5’-

CGCCGCCGCCGTGGAGAGTCTCAT-3' (Lewis et al., 2005); *shha* MO: 5'-CAGCACTCTCGTCAAAAGCCGCATT-3' (Nasevicius and Ekker, 2000). The specificity of the *sox4* morphant phenotypes was confirmed with a second, non-overlapping set of *sox4* morpholinos (*sox4a* MO2: 5'-CAACAGTCTCAACTTTTAATTGCGC-3'; *sox4b* MO2: 5'-GAGACTCAGTCTGATTGCAGCACAC-3'). Embryos were injected with 5.3 ng each of *sox4a* MO1 and *sox4b* MO1, 10.5 ng each of *sox4a* MO2 and *sox4b* MO2, or 10.5 ng of standard control MO. Both *sox4* MO1 and MO2 generated similar phenotypes. Unless stated otherwise, all data presented in this study were from embryos injected with *sox4a* MO1 and *sox4b* MO1. A p53 morpholino (Robu et al., 2007) was co-injected (at 1.5-fold the amount of *sox4* MOs) to suppress cell death (p53 MO 5'-GCGCCATTGCTTTGCAAGAATTG-3').

To determine the efficiency of the *sox4* MOs, PCR fragments corresponding to the 5' UTRs of *sox4a* and *sox4b* mRNA and containing the *sox4a* MO and *sox4b* MO target sequence, respectively, were amplified and cloned upstream and in frame with the GFP gene in the *pEF1α:GFP* plasmid (Addgene, Cambridge, MA). One-cell stage zebrafish embryos were injected with 50 pg/embryo of *pEF1α-sox4a MO:GFP* and 50 pg/embryo of *pEF1α-sox4b MO:GFP* plasmids in the presence or absence of *sox4a* MO1 and/or *sox4b* MO1. GFP expression in injected embryos was analyzed by fluorescence microscopy at 24 hpf.

For mRNA rescue and overexpression experiments, the zebrafish *sox4a/b* and *sox11a/b* coding sequences (lacking the MO target sites) were PCR amplified from 48 hpf complimentary DNA (cDNA) and cloned into the pGEM-T-easy vector (Promega, Madison, WI). The capped mRNAs were synthesized with the mMessage mMACHINE transcription kit (Life Technologies, Carlsbad, CA) according to the manufacturer's instructions. Control *Td-tomato* mRNA was synthesized from *pRSET-B-td-Tomato* (kindly provided by D.A. Harrison, University of Kentucky, Lexington, KY). For mRNA rescue experiments, 0.5 ng/embryo of *sox4a* and *sox4b* mRNA or 1.0 ng/embryo of *sox11a* and *sox11b* mRNA was co-injected with the *sox4a/b* MOs. For mRNA overexpression experiments, 0.5 ng/embryo of *sox4a* and *sox4b* mRNA or an equimolar amount of *Td-tomato* mRNA was injected into wild type embryos. Alternatively, a total of 1 ng of mRNA containing different ratios of control *Td-Tomato* and *sox4* mRNA was injected. *Bmp7b* mRNA was synthesized from a *pCRII-bmp7b* plasmid (a kind gift from Dr. S. Fabrizio, The Novartis Institutes for Biomedical Research, Cambridge, MA). 1.0 ng/embryo of *bmp7b* mRNA was injected into *sox4* morphants.

CRISPR sgRNA and Cas9 mRNA synthesis and injection

Sox4a and *sox4b* CRISPR target sites were identified and the corresponding sgRNA oligos were designed using the ZiFiT online software (www.zifit.partners.org/ZiFiT/; Table S1). Oligo pairs (100μM) for each sgRNA were mixed with NEBuffer4 (New England Biolabs, lpswich, MA), incubated in boiling water for 5 minutes, followed by 2 hours annealing at room temperature, and then ligated with linearized pDR274 vector (Addgene, Cambridge, MA) at 16°C overnight. Recombinant plasmid was digested with DraI to drop out the sgRNA template, followed by PCR amplification (Table S1) using the KOD Hot Start Master Mix (Millipore, Billerica, MA) and purification using QIAquick PCR Purification

Kit (Qiagen, Valencia, CA). sgRNA was generated using the MEGAscript T7 Transcription Kit (Life Technologies, Carlsbad, CA). To prepare the *tyr* sgRNA, pT7tyrgRNA (Addgene, Cambridge, MA) was linearized with BamHI and sgRNA was synthesized using MEGAscript T7 Transcription Kit (Life Technologies). To generate the Cas9 mRNA, *pCS2-nCas9n* plasmid (Addgene, Cambridge, MA) was linearized with NotI and capped *Cas9* mRNA was synthesized using the mMESSAGE mMACHINE SP6 Transcription Kit (Life Technologies). To confirm the quality of sgRNA and *Cas9* mRNA, RNA was mixed with formamide, heated at 72°C for 5 minutes and run on a 1% (wt/vol) agarose gel. The following sgRNA and *Cas9* mRNA doses were microinjected into embryos at the one-cell stage: 100 pg/embryo of *sox4a* or *sox4b* sgRNA + 200 pg/embryo of *Cas9* mRNA; 50 pg/embryo of *tyr* sgRNA + 150 pg/embryo of *Cas9* mRNA.

HRMA analysis

To isolate genomic DNA from uninjected or sgRNA/Cas9 injected individual embryos, 24 hpf dechorionated embryos were placed into individual wells of a 96-well plate containing 20 µl of 1X ThermoPol Buffer (New England Biolabs, lpswich, MA). The plate was placed in a PCR cycler at 95°C for 10 minutes, after which 5 µl of 10 mg/ml Proteinase K (Sigma, St. Louis, MO) was added to each well and the plate was incubated at 55°C for 1 hour and 95°C for 10 minutes. HRMA analysis was performed on a LightCycler 96 Real-Time PCR System (Roche, Indianapolis, IN) using LightCycler 480 High Resolution Melting Master (Roche), following the manufacturer's instructions. Primer sequences used for HRMA are listed in Table S1.

Immunohistochemistry and TUNEL assay

Immunohistochemistry was performed on cryosections or whole zebrafish embryos as previously described (Fadool, 2003; Forbes-Osborne et al., 2013). Images were obtained on an inverted fluorescent microscope (Eclipse Ti-U; Nikon Instruments) using the 20X objective. The following primary antibodies and dilutions were used: anti-PCNA (mouse, 1:100, Santa Cruz Biotechnology, Dallas, Texas), which labels cells in G1/S phase; anti-PH3 (rabbit, 1:500, Millipore, Billerica, MA), which labels cells in G2/M phase; anti-Zn-8 (mouse, 1:10, ZIRC, Eugene, OR), which labels ganglion cells; anti-Prox1 (rabbit, 1:1000, Acris, San Diego, CA), which recognizes horizontal cells; anti-PKCα (rabbit, 1:100, Santa Cruz Biotechnology, Dallas, Texas), which labels bipolar cells. Alexa fluor-conjugated secondary antibodies (Invitrogen, Grand Island, NY) and Cy-conjugated secondary antibodies (Jackson ImmunoResearch, West Grove, PA) were all used at a dilution of 1:200. Sections were counterstained with DAPI (1:10,000, Sigma, St. Louis, MO) to visualize cell nuclei. For laminin immunostaining, 48 and 72 hpf zebrafish embryos were hybridized with anti-laminin (mouse, 1:60, Sigma, St. Louis, MO), and imaged on a laser scanning confocal microscope (Leica TCS SP5). TUNEL assay was performed on retinal cryosections using the ApopTag Fluorescein Direct In Situ Apoptosis Detection Kit (Millipore, Billerica, MA) according to the manufacturer's instructions.

Real-Time quantitative RT-PCR

Total RNA was extracted from the whole body of control and *sox4* morphant embryos at 8, 10, and 12 hpf or the heads of control and *sox4* morphant embryos, or *TdTomato* and *sox4* mRNA injected embryos, at 18 and 24 hpf using TRIzol reagent (Invitrogen, Grand Island, NY). RNA was reverse-transcribed using the GoScript Reverse Transcriptase System (Promega, Madison, WI). Real time PCR was performed using Maxima SYBR Green qPCR master mix (Thermo Scientific, Waltham, MA) on an iCycler iQ Real Time PCR Detection system (Bio-Rad, Hercules, CA), or using FastStart Essential DNA Green Master (Roche, Indianapolis, IN) on a LightCycler 96 Real-Time PCR System (Roche, Indianapolis, IN). For all experiments, three biological replicates were analyzed, and relative transcript abundance was normalized to expression of the housekeeping genes *gapdh* or *atp5h*.

Cyclopamine treatments

Cyclopamine (Sigma, St. Louis, MO) was resuspended at 1mM in 100% ethanol and diluted with fish water to a final concentration of 0.2 μM. For vehicle controls, 0.2% ethanol in fish water was used. Embryos injected with standard control MO or *sox4* MOs were exposed to cyclopamine or ethanol from 5.5 to 13 hpf and then placed into fresh fish water until 24 hpf.

SDS PAGE and Western blots

Protein was extracted from pools of 80-100 24 hpf control and *sox4* morphant heads. Protein concentrations were measured using the Pierce BCA Protein Assay Kit (Thermo Scientific, Waltham, MA). Ten μg of total protein per sample was diluted 1:1 with Laemmli buffer and 2.5% β-mercaptoethanol, boiled for 10 minutes, and then separated by SDS-PAGE on 10% polyacrylamide gels. Resolved proteins were transferred to nitrocellulose membranes and blocked in 1X TBS/0.05% TWEEN/5% BSA for 1 hour at room temperature prior to incubation with either anti-IHH antibody (rabbit polyclonal, 1:800, Sigma, St. Louis, MO), or anti-β-Actin (rabbit polyclonal, 1:2000, Abcam, Cambridge, MA) as a loading control. The IHH antibody immunogen sequence partially overlaps with zebrafish Ihha, Ihhb and Shhb protein sequences. Membranes were washed and incubated in goat anti-rabbit-peroxidase secondary antibody (1:3000, Sigma, St. Louis, MO). Blots were developed using the Pierce ECL Western Blotting Substrate (Thermo Scientific, Waltham, MA) according to the manufacturer's instructions.

Statistical Analyses

Significance was calculated using a two-tailed Student's *t*-test or Fisher's exact test, with $P<0.05$ being considered significant. For all graphs, data are represented as the mean ± the standard deviation (s.d.).

Supplementary Material

Refer to Web version on PubMed Central for supplementary material.

ACKNOWLEDGEMENTS

The authors would like to thank Sara Perkins for zebrafish care, and Marie Forbes-Osborne, Joanna Ng, Abirami Krishna, and the laboratory of Dr. Vincent Cassone and Dr. Ashley Seifert for technical assistance. The authors

would also like to give special thanks to Dr. Jared C. Talbot (S. Amacher lab, Ohio State University, Columbus, OH) and Dr. Jeffrey J. Essner (Iowa State University, Ames, IA) for sharing their CRISPR protocols.

FUNDING

This work was supported by a grant from the National Institutes of Health (R01EY021769, A.C.M.), the Pew Biomedical Scholar Program (A.C.M.), and the Lyman T. Johnson and Academic Year graduate fellowships from the University of Kentucky (W.W. and L.P.K.).

REFERENCES

Amato MA, Boy S, Perron M. Hedgehog signaling in vertebrate eye development: a growing puzzle. Cellular and molecular life sciences : CMLS. 2004; 61:899–910. [PubMed: 15095011]

Bassett EA, Williams T, Zacharias AL, Gage PJ, Fuhrmann S, West-Mays JA. AP-2alpha knockout mice exhibit optic cup patterning defects and failure of optic stalk morphogenesis. Human molecular genetics. 2010; 19:1791–1804. [PubMed: 20150232]

Bastida MF, Sheth R, Ros MA. A BMP-Shh negative-feedback loop restricts Shh expression during limb development. Development (Cambridge, England). 2009; 136:3779–3789.

Bergsland M, Werme M, Malewicz M, Perlmann T, Muhr J. The establishment of neuronal properties is controlled by Sox4 and Sox11. Genes Dev. 2006; 20:3475–3486. [PubMed: 17182872]

Bernardos RL, Barthel LK, Meyers JR, Raymond PA. Late-stage neuronal progenitors in the retina are radial Muller glia that function as retinal stem cells. The Journal of neuroscience : the official journal of the Society for Neuroscience. 2007; 27:7028–7040. [PubMed: 17596452]

Bhattaram P, Penzo-Mendez A, Sock E, Colmenares C, Kaneko KJ, Vassilev A, Depamphilis ML, Wegner M, Lefebvre V. Organogenesis relies on SoxC transcription factors for the survival of neural and mesenchymal progenitors. Nature communications. 2010; 1:9.

Bibliowicz J, Gross JM. Ectopic proliferation contributes to retinal dysplasia in the juvenile zebrafish patched2 mutant eye. Investigative ophthalmology & visual science. 2011; 52:8868–8877. [PubMed: 22003118]

Bowles J, Schepers G, Koopman P. Phylogeny of the SOX family of developmental transcription factors based on sequence and structural indicators. Developmental biology. 2000; 227:239–255. [PubMed: 11071752]

Briscoe J, Therond PP. The mechanisms of Hedgehog signalling and its roles in development and disease. Nature reviews. Molecular cell biology. 2013; 14:416–429.

Cai J, Xu X, Yin H, Wu R, Modderman G, Chen Y, Jensen J, Hui CC, Qiu M. Evidence for the differential regulation of Nkx-6.1 expression in the ventral spinal cord and foregut by Shh-dependent and -independent mechanisms. Genesis. 2000; 27:6–11. [PubMed: 10862150]

Cepko CL, Austin CP, Yang X, Alexiades M, Ezzeddine D. Cell fate determination in the vertebrate retina. Proceedings of the National Academy of Sciences of the United States of America. 1996; 93:589–595. [PubMed: 8570600]

Chang L, Blain D, Bertuzzi S, Brooks BP. Uveal coloboma: clinical and basic science update. Current opinion in ophthalmology. 2006; 17:447–470. [PubMed: 16932062]

Cheung M, Abu-Elmagd M, Clevers H, Scotting PJ. Roles of Sox4 in central nervous system development. Brain research. Molecular brain research. 2000; 79:180–191. [PubMed: 10925158]

Chung AY, Kim S, Kim E, Kim D, Jeong I, Cha YR, Bae YK, Park SW, Lee J, Park HC. Indian hedgehog B function is required for the specification of oligodendrocyte progenitor cells in the zebrafish CNS. The Journal of neuroscience : the official journal of the Society for Neuroscience. 2013; 33:1728–1733. [PubMed: 23345245]

Currie PD, Ingham PW. Induction of a specific muscle cell type by a hedgehog-like protein in zebrafish. Nature. 1996; 382:452–455. [PubMed: 8684485]

Dakubo GD, Mazerolle C, Furimsky M, Yu C, St-Jacques B, McMahon AP, Wallace VA. Indian hedgehog signaling from endothelial cells is required for sclera and retinal pigment epithelium development in the mouse eye. Developmental biology. 2008; 320:242–255. [PubMed: 18582859]

Duench K, Franz-Odendaal TA. BMP and Hedgehog signaling during the development of scleral ossicles. Developmental biology. 2012; 365:251–258. [PubMed: 22370003]

Dy P, Penzo-Mendez A, Wang H, Pedraza CE, Macklin WB, Lefebvre V. The three SoxC proteins--Sox4, Sox11 and Sox12--exhibit overlapping expression patterns and molecular properties. Nucleic acids research. 2008; 36:3101–3117. [PubMed: 18403418]

Eccles MR, Schimmenti LA. Renal-coloboma syndrome: a multi-system developmental disorder caused by PAX2 mutations. Clinical genetics. 1999; 56:1–9. [PubMed: 10466411]

Ekker SC, Ungar AR, Greenstein P, von Kessler DP, Porter JA, Moon RT, Beachy PA. Patterning activities of vertebrate hedgehog proteins in the developing eye and brain. Current biology : CB. 1995; 5:944–955. [PubMed: 7583153]

Fadool JM. Development of a rod photoreceptor mosaic revealed in transgenic zebrafish. Developmental biology. 2003; 258:277–290. [PubMed: 12798288]

Feng W, Khan MA, Bellvis P, Zhu Z, Bernhardt O, Herold-Mende C, Liu HK. The chromatin remodeler CHD7 regulates adult neurogenesis via activation of SoxC transcription factors. Cell stem cell. 2013; 13:62–72. [PubMed: 23827709]

Flandin P, Zhao Y, Vogt D, Jeong J, Long J, Potter G, Westphal H, Rubenstein JL. Lhx6 and Lhx8 coordinately induce neuronal expression of Shh that controls the generation of interneuron progenitors. Neuron. 2011; 70:939–950. [PubMed: 21658586]

Forbes-Osborne MA, Wilson SG, Morris AC. Insulinoma-associated 1a (Insm1a) is required for photoreceptor differentiation in the zebrafish retina. Developmental. 2013; 380:157–171.

Gongal PA, French CR, Waskiewicz AJ. Aberrant forebrain signaling during early development underlies the generation of holoprosencephaly and coloboma. Biochimica et biophysica acta. 2011; 1812:390–401. [PubMed: 20850526]

Gregory-Evans CY, Williams MJ, Halford S, Gregory-Evans K. Ocular coloboma: a reassessment in the age of molecular neuroscience. Journal of medical genetics. 2004; 41:881–891. [PubMed: 15591273]

Guirgis MF, Lueder GT. Choroidal neovascular membrane associated with optic nerve coloboma in a patient with CHARGE association. American journal of ophthalmology. 2003; 135:919–920. [PubMed: 12788148]

Hammerschmidt M, Bitgood MJ, McMahon AP. Protein kinase A is a common negative regulator of Hedgehog signaling in the vertebrate embryo. Genes & Development. 1996; 10:647–658. [PubMed: 8598293]

Hoffman TL, Javier AL, Campeau SA, Knight RD, Schilling TF. Tfap2 transcription factors in zebrafish neural crest development and ectodermal evolution. Journal of experimental zoology. Part B, Molecular and developmental evolution. 2007; 308:679–691.

Hornby SJ, Gilbert CE, Rahi JK, Sil AK, Xiao Y, Dandona L, Foster A. Regional variation in blindness in children due to microphthalmos, anophthalmos and coloboma. Ophthalmic epidemiology. 2000; 7:127–138. [PubMed: 10934463]

Hruscha A, Krawitz P, Rechenberg A, Heinrich V, Hecht J, Haass C, Schmid B. Efficient CRISPR/Cas9 genome editing with low off-target effects in zebrafish. Development (Cambridge, England. 2013; 140:4982–4987.

Hwang WY, Fu Y, Reyon D, Maeder ML, Tsai SQ, Sander JD, Peterson RT, Yeh JR, Joung JK. Efficient genome editing in zebrafish using a CRISPR-Cas system. Nature biotechnology. 2013; 31:227–229.

Ingham PW, McMahon AP. Hedgehog signaling in animal development: paradigms and principles. Genes Dev. 2001; 15:3059–3087. [PubMed: 11731473]

Jao LE, Wente SR, Chen W. Efficient multiplex biallelic zebrafish genome editing using a CRISPR nuclease system. Proceedings of the National Academy of Sciences of the United States of America. 2013; 110:13904–13909. [PubMed: 23918387]

Jiang Y, Ding Q, Xie X, Libby RT, Lefebvre V, Gan L. Transcription factors SOX4 and SOX11 function redundantly to regulate the development of mouse retinal ganglion cells. The Journal of biological chemistry. 2013; 288:18429–18438. [PubMed: 23649630]

Kim TH, Goodman J, Anderson KV, Niswander L. Phactr4 regulates neural tube and optic fissure closure by controlling PP1-, Rb-, and E2F1-regulated cell-cycle progression. Developmental cell. 2007; 13:87–102. [PubMed: 17609112]

Kimmel CB, Ballard WW, Kimmel SR, Ullmann B, Schilling TF. Stages of embryonic development of the zebrafish. Developmental dynamics : an official publication of the American Association of Anatomists. 1995; 203:253–310. [PubMed: 8589427]

Kosinski C, Stange DE, Xu C, Chan AS, Ho C, Yuen ST, Mifflin RC, Powell DW, Clevers H, Leung SY, et al. Indian hedgehog regulates intestinal stem cell fate through epithelial-mesenchymal interactions during development. Gastroenterology. 2010; 139:893–903. [PubMed: 20542037]

Lee J, Willer JR, Willer GB, Smith K, Gregg RG, Gross JM. Zebrafish blowout provides genetic evidence for Patched1-mediated negative regulation of Hedgehog signaling within the proximal optic vesicle of the vertebrate eye. Developmental biology. 2008; 319:10–22. [PubMed: 18479681]

Lee J, Cox BD, Daly CM, Lee C, Nuckels RJ, Tittle RK, Uribe RA, Gross JM. An ENU mutagenesis screen in zebrafish for visual system mutants identifies a novel splice-acceptor site mutation in patched2 that results in Colobomas. Investigative ophthalmology & visual science. 2012; 53:8214–8221. [PubMed: 23150614]

Lewis KE, Bates J, Eisen JS. Regulation of iro3 expression in the zebrafish spinal cord. Developmental dynamics : an official publication of the American Association of Anatomists. 2005; 232:140–148. [PubMed: 15580554]

Liu C, Bakeri H, Li T, Swaroop A. Regulation of retinal progenitor expansion by Frizzled receptors: implications for microphthalmia and retinal coloboma. Human molecular genetics. 2012; 21:1848–1860. [PubMed: 22228100]

Locker M, Agathocleous M, Amato MA, Parain K, Harris WA, Perron M. Hedgehog signaling and the retina: insights into the mechanisms controlling the proliferative properties of neural precursors. Genes Dev. 2006; 20:3036–3048. [PubMed: 17079690]

Manning L, Ohyama K, Saeger B, Hatano O, Wilson SA, Logan M, Placzek M. Regional morphogenesis in the hypothalamus: a BMP-Tbx2 pathway coordinates fate and proliferation through Shh downregulation. Developmental cell. 2006; 11:873–885. [PubMed: 17141161]

Marti E, Bovolenta P. Sonic hedgehog in CNS development: one signal, multiple outputs. Trends in neurosciences. 2002; 25:89–96. [PubMed: 11814561]

Mavropoulos A, Devos N, Biemar F, Zecchin E, Argenton F, Edlund H, Motte P, Martial JA, Peers B. sox4b is a key player of pancreatic alpha cell differentiation in zebrafish. Developmental biology. 2005; 285:211–223. [PubMed: 16055112]

Morcillo J, Martinez-Morales JR, Trousse F, Fermin Y, Sowden JC, Bovolenta P. Proper patterning of the optic fissure requires the sequential activity of BMP7 and SHH. Development (Cambridge, England). 2006; 133:3179–3190.

Morris AC, Forbes-Osborne MA, Pillai LS, Fadool JM. Microarray analysis of XOPS-mCFP zebrafish retina identifies genes associated with rod photoreceptor degeneration and regeneration. Investigative ophthalmology & visual science. 2011; 52:2255–2266. [PubMed: 21217106]

Morrison DA, FitzPatrick DR, Fleck BW. Iris coloboma with iris heterochromia: a common association. Archives of ophthalmology. 2000; 118:1590–1591. [PubMed: 11074823]

Moshiri A, Reh TA. Persistent progenitors at the retinal margin of ptc+/−mice. The Journal of neuroscience : the official journal of the Society for Neuroscience. 2004; 24:229–237. [PubMed: 14715955]

Mukhopadhyay A, Krishnaswami SR, Cowing-Zitron C, Hung NJ, Reilly-Rhoten H, Burns J, Yu BD. Negative regulation of Shh levels by Kras and Fgfr2 during hair follicle development. Developmental biology. 2013; 373:373–382. [PubMed: 23123965]

Nasevicius A, Ekker SC. Effective targeted gene ‘knockdown’ in zebrafish. Nature genetics. 2000; 26:216–220. [PubMed: 11017081]

Nelson SM, Frey RA, Wardwell SL, Stenkamp DL. The developmental sequence of gene expression within the rod photoreceptor lineage in embryonic zebrafish. Developmental dynamics : an official publication of the American Association of Anatomists. 2008; 237:2903–2917. [PubMed: 18816851]

Ochocinska MJ, Hitchcock PF. Dynamic expression of the basic helix-loop-helix transcription factor neuroD in the rod and cone photoreceptor lineages in the retina of the embryonic and larval zebrafish. The Journal of comparative neurology. 2007; 501:1–12. [PubMed: 17206615]

Pathi S, Rutenberg JB, Johnson RL, Vortkamp A. Interaction of Ihh and BMP/Noggin signaling during cartilage differentiation. Developmental biology. 1999; 209:239–253. [PubMed: 10328918]

Paul MH, Harvey RP, Wegner M, Sock E. Cardiac outflow tract development relies on the complex function of Sox4 and Sox11 in multiple cell types. Cellular and molecular life sciences : CMLS. 2013

Penzo-Mendez AI. Critical roles for SoxC transcription factors in development and cancer. The international journal of biochemistry & cell biology. 2010; 42:425–428. [PubMed: 19651233]

Pillai-Kastoori L, Wen W, Wilson SG, Strachan E, Lo-Castro A, Fichera M, Musumeci SA, Lehmann OJ, Morris AC. Sox11 Is Required to Maintain Proper Levels of Hedgehog Signaling during Vertebrate Ocular Morphogenesis. PLoS genetics. 2014; 10:e1004491. [PubMed: 25010521]

Porges Y, Gershoni-Baruch R, Leibu R, Goldscher D, Zonis S, Shapira I, Miller B. Hereditary microphthalmia with colobomatous cyst. American journal of ophthalmology. 1992; 114:30–34. [PubMed: 1621783]

Robu ME, Larson JD, Nasevicius A, Beiraghi S, Brenner C, Farber SA, Ekker SC. p53 activation by knockdown technologies. PLoS genetics. 2007; 3:e78. [PubMed: 17530925]

Sanyanusin P, Schimmenti LA, McNoe LA, Ward TA, Pierpont ME, Sullivan MJ, Dobyns WB, Eccles MR. Mutation of the PAX2 gene in a family with optic nerve colobomas, renal anomalies and vesicoureteral reflux. Nature genetics. 1995; 9:358–364. [PubMed: 7795640]

Schauerte HE, van Eeden FJ, Fricke C, Odenthal J, Strahle U, Haffter P. Sonic hedgehog is not required for the induction of medial floor plate cells in the zebrafish. Development (Cambridge, England). 1998; 125:2983–2993.

Schilham MW, Oosterwegel MA, Moerer P, Ya J, de Boer PA, van de Wetering M, Verbeek S, Lamers WH, Kruisbeek AM, Cumano A, et al. Defects in cardiac outflow tract formation and pro-B-lymphocyte expansion in mice lacking Sox-4. Nature. 1996; 380:711–714. [PubMed: 8614465]

Schimmenti LA, de la Cruz J, Lewis RA, Karkera JD, Manligas GS, Roessler E, Muenke M. Novel mutation in sonic hedgehog in non-syndromic colobomatous microphthalmia. American journal of medical genetics. Part A. 2003; 116A:215–221. [PubMed: 12503095]

Seki K, Hata A. Indian hedgehog gene is a target of the bone morphogenetic protein signaling pathway. The Journal of biological chemistry. 2004; 279:18544–18549. [PubMed: 14981086]

Shen MC, Ozacar AT, Osgood M, Boeras C, Pink J, Thomas J, Kohtz JD, Karlstrom R. Heat-shock-mediated conditional regulation of hedgehog/gli signaling in zebrafish. Developmental dynamics : an official publication of the American Association of Anatomists. 2013; 242:539–549. [PubMed: 23441066]

Shen YC, Raymond PA. Zebrafish cone-rod (crx) homeobox gene promotes retinogenesis. Developmental biology. 2004; 269:237–251. [PubMed: 15081370]

Slavotinek AM, Chao R, Vacik T, Yahyavi M, Abouzeid H, Bardakjian T, Schneider A, Shaw G, Sherr EH, Lemke G, et al. VAX1 mutation associated with microphthalmia, corpus callosum agenesis, and orofacial clefting: the first description of a VAX1 phenotype in humans. Human mutation. 2012; 33:364–368. [PubMed: 22095910]

St-Jacques B, Hammerschmidt M, McMahon AP. Indian hedgehog signaling regulates proliferation and differentiation of chondrocytes and is essential for bone formation. Genes Dev. 1999; 13:2072–2086. [PubMed: 10465785]

Stenkamp DL. Neurogenesis in the Fish Retina. 2007; 259:173–224.

Take-uchi M. Hedgehog signalling maintains the optic stalk-retinal interface through the regulation of Vax gene activity. Development (Cambridge, England). 2003; 130:955–968.

Talbot JC, Amacher SL. A Streamlined CRISPR Pipeline to Reliably Generate Zebrafish Frameshifting Alleles. Zebrafish. 2014; 11:583–585. [PubMed: 25470533]

Usui A, Iwagawa T, Mochizuki Y, Iida A, Wegner M, Murakami A, Watanabe S. Expression of Sox4 and Sox11 is regulated by multiple mechanisms during retinal development. FEBS letters. 2013; 587:358–363. [PubMed: 23313252]

van de Wetering M, Oosterwegel M, van Norren K, Clevers H. Sox-4, an Sry-like HMG box protein, is a transcriptional activator in lymphocytes. The EMBO journal. 1993; 12:3847–3854. [PubMed: 8404853]

Westerfield, M. The zebrafish book. A guide for the laboratory use of zebrafish (Danio rerio). 4th ed.. Univ. of Oregon Press; Eugene: 2000.

Wolff C, Roy S, Ingham PW. Multiple Muscle Cell Identities Induced by Distinct Levels and Timing of Hedgehog Activity in the Zebrafish Embryo. Current Biology. 2003; 13:1169–1181. [PubMed: 12867027]

Yen ST, Zhang M, Deng JM, Usman SJ, Smith CN, Parker-Thornburg J, Swinton PG, Martin JF, Behringer RR. Somatic mosaicism and allele complexity induced by CRISPR/Cas9 RNA injections in mouse zygotes. Developmental biology. 2014; 393:3–9. [PubMed: 24984260]

Zhang D, Golubkov VS, Han W, Correa RG, Zhou Y, Lee S, Strongin AY, Dong PD. Identification of Annexin A4 as a hepatopancreas factor involved in liver cell survival. Developmental biology. 2014; 395:96–110. [PubMed: 25176043]

Zhang R, Huang H, Cao P, Wang Z, Chen Y, Pan Y. Sma-and Mad-related protein 7 (Smad7) is required for embryonic eye development in the mouse. The Journal of biological chemistry. 2013; 288:10275–10285. [PubMed: 23426374]

HIGHLIGHTS

- Sox4 is required for choroid fissure closure, and Sox4 deficiency causes ocular coloboma.
- Knockdown of Sox4 alters proximo-distal patterning of the optic stalk and vesicle.
- Knockdown of Sox4 results in elevated Hh signaling.
- Sox4 negatively regulates expression of the Hh ligand gene *indian hedgehog* (*ihhb*).

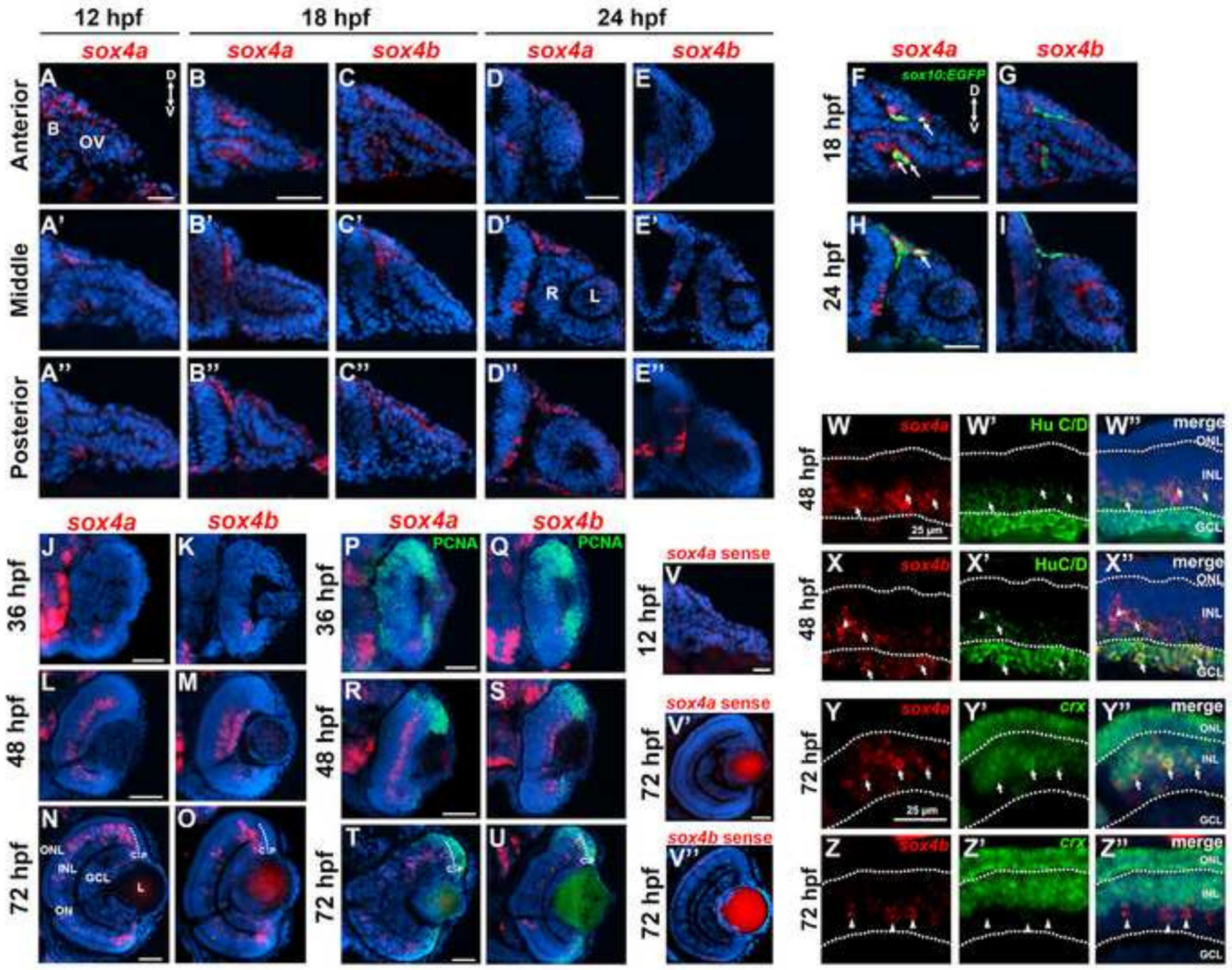

Figure 1. Expression of *sox4a* and *sox4b* during ocular development

(A-A") Fluorescent in situ hybridization (FISH) for *sox4a* performed on transverse cryosections at 12 hpf. (B-D") FISH for *sox4a* (B-B" and D-D") or *sox4b* (C-C" and E-E") performed on transverse cryosections taken at the level of the anterior, middle, and posterior optic vesicle at 18 or 24 hpf. (F-I) FISH with *sox4a* and *sox4b* probes performed on sections from *sox10*:*EGFP* transgenic embryos at 18 and 24 hpf . (J-O) FISH for *sox4a* or *sox4b* performed on transverse retinal cryosections at 36, 48, and 72 hpf. (P-U) FISH combined with immunohistochemistry for the proliferation marker PCNA at 24, 48, or 72 hpf. (V-V") Control FISH with a sense probe for *sox4a* and *sox4b* at 12 and 72 hpf. (W-X") FISH combined with immunohistochemistry for HuC/D, which labels ganglion and amacrine cells, at 48 hpf. (Y-Z") Two-color FISH with *sox4a/b* and *crx* probes performed at 72 hpf. Arrows indicate co-localization, arrowheads indicate *sox4a/b*+ cells that did not co-localize with the indicated marker. All scale bars equal 50 μm. D, dorsal; V, ventral; B, brain; OV, optic vesicle; L, lens; R, retina; P, peripheral CMZ; C, central CMZ; GCL, ganglion cell layer; INL, inner nuclear layer; ONL, outer nuclear layer; ON, optic nerve.

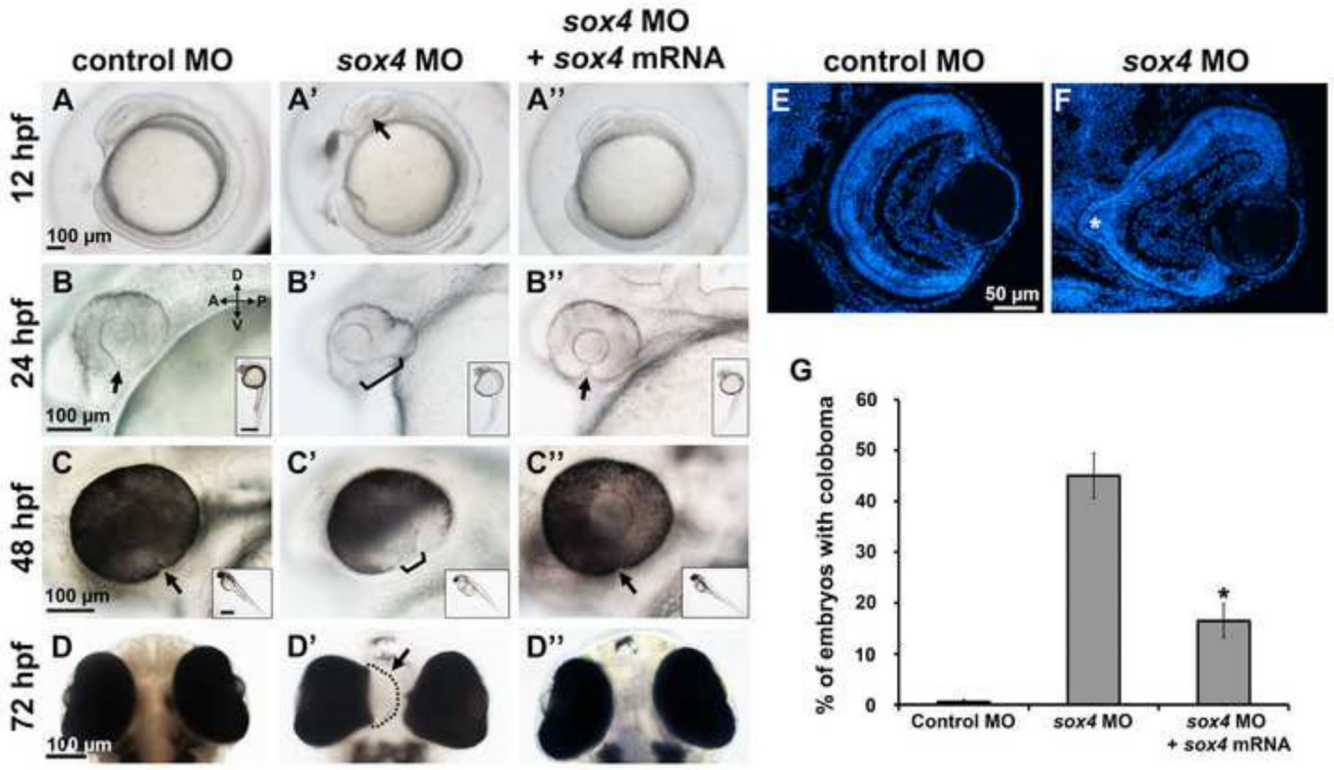

Figure 2. Knockdown of *sox4* causes coloboma

Representative images of control MO-injected embryos (A-D), *sox4* MO-injected embryos (A'-D'), and embryos injected with both *sox4* MO and *sox4* mRNA (A"-D"). A minimum of 5 embryos were imaged for each group. Images in A-C" are lateral views; images in D-D" were taken from the ventral side of the embryo. Insets show the whole body of the same embryo in the larger panel. Arrow in A' indicates the horizontal crease; arrows and brackets in B-C" indicate the choroid fissure. (E-F) Transverse DAPI-stained sections of control and *sox4* morphants at 72 hpf. The coloboma in the *sox4* morphant retina is prominent (F, asterisk). (G) Quantification of the coloboma phenotype at 48 hpf. In control morphants, 0.61± 0.49% of embryos displayed coloboma (n= 2/329). In *sox4* morphants, 45.01± 4.43% of embryos displayed coloboma (n= 257/571). Co-injection of *sox4* mRNA significantly reduced the incidence of coloboma to 16.49± 3.37% (n= 31/188; Fisher's exact test, P< 0.0001).Scale bars for the insets in B-C" equal 500 µm.

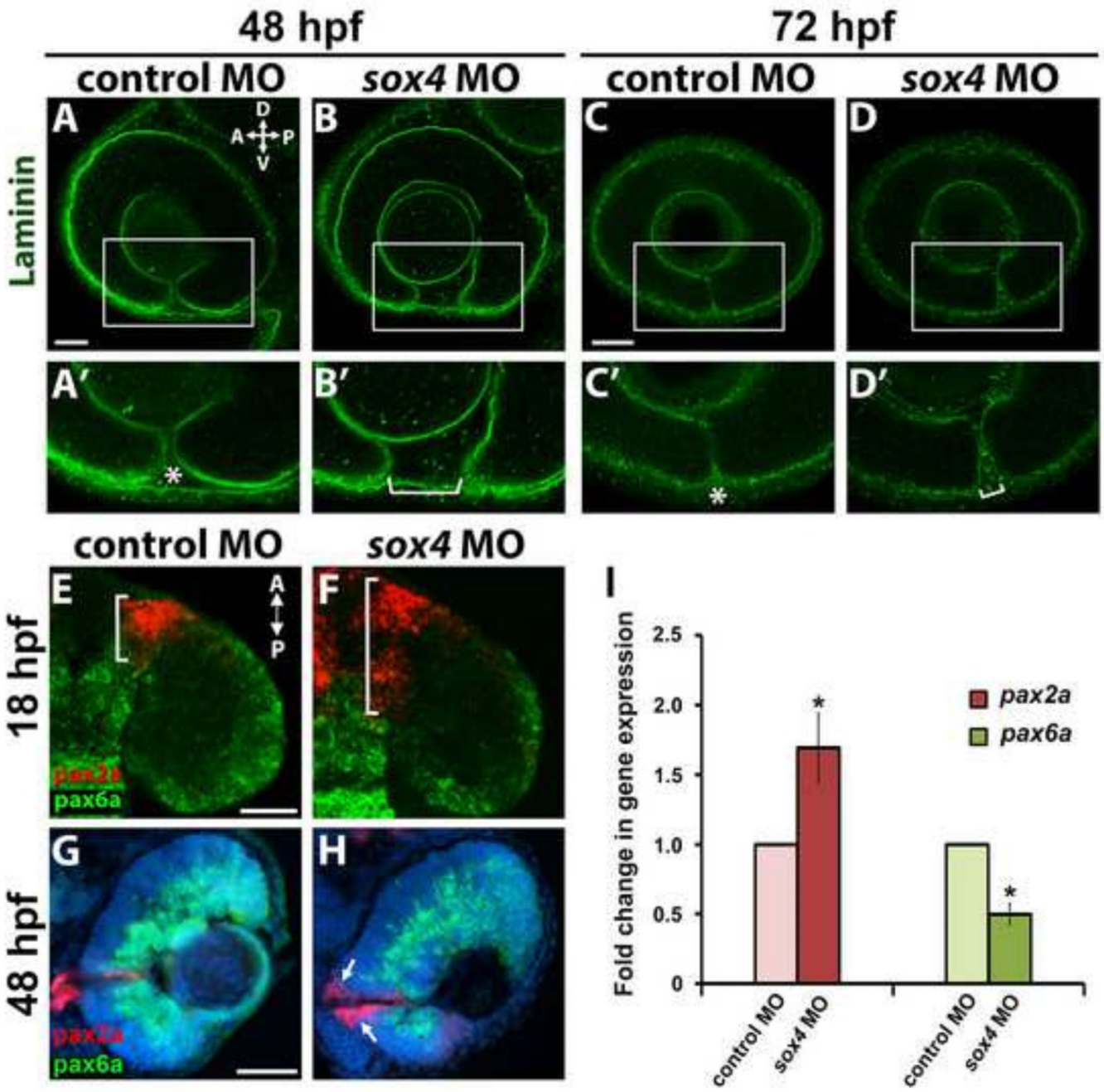

Figure 3. Persistence of laminin expression at the choroid fissure and altered proximo-distal patterning of the optic vesicle in *sox4* morphants

(A-D') Laminin immunostaining on control and *sox4* morphant embryos at 48 and 72 hpf. Representative images from 15-20 individuals analyzed for each group are shown. (E-H) Double FISH for *pax2a* and *pax6a* at 18 and 48 hpf. (I) qPCR analysis revealed a 1.69-fold increase in *pax2a* expression and a 2.0-fold decrease in *pax6a* expression in *sox4* morphant heads at 18 hpf (Student's *t*-test, $P<0.05$). All scale bars equal 50 μm. Asterisks in A' and C' indicate the closing or fused choroid fissure in control morphants; brackets in B' and D' indicate the open choroid fissure in *sox4* morphants.

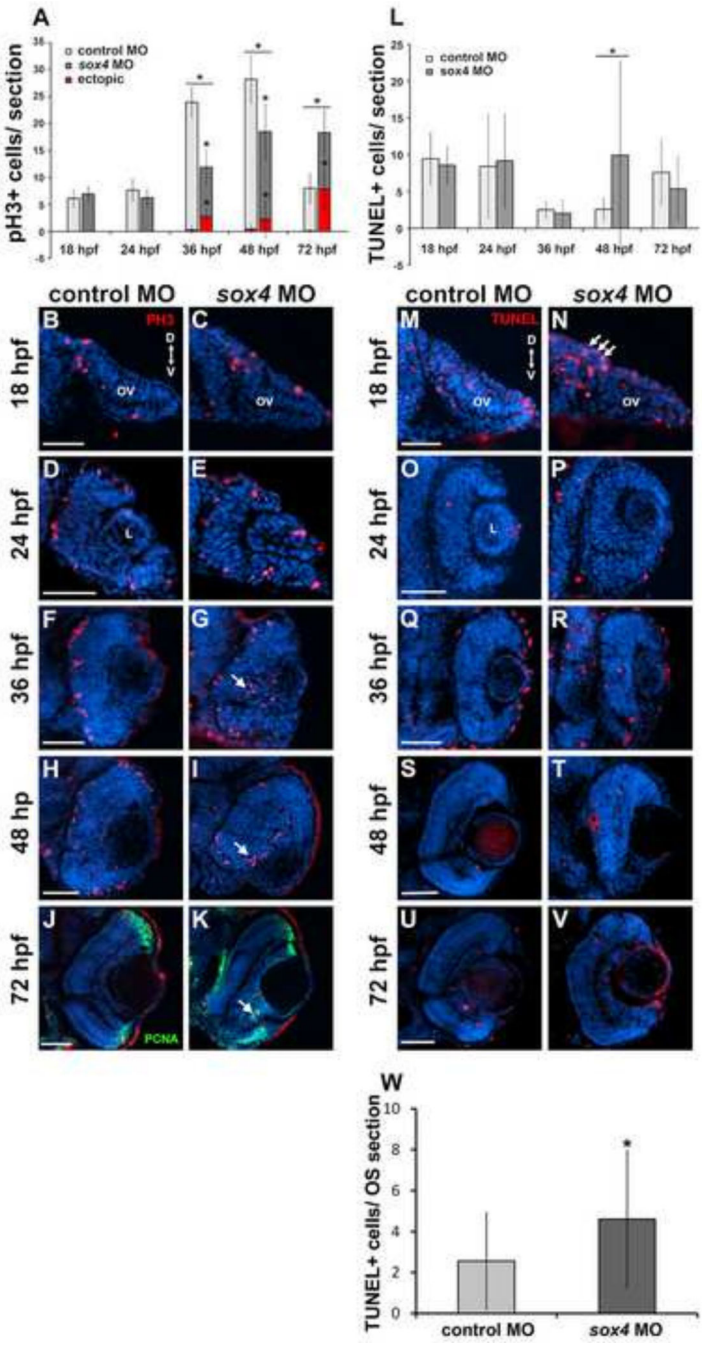

Figure 4. *Sox4* knockdown causes ectopic cell proliferation in the retina

(A) Quantification of PH3-positive cells in control and *sox4* morphant retinas from 18 to 72 hpf. 8-10 individuals were analyzed in each time point (Student's *t*-test, P< 0.01). (B-K) Representative transverse sections through the optic vesicle and retina of control and *sox4* morphants immunolabeled for PH3 at the indicated time points. Ectopic PH3-positive cells are indicated by arrows. At 72 hpf, the ectopic PH3-positive cells in the GCL also clustered with PCNA-positive cells (K, arrow). (L) Quantification of TUNEL-positive cells in control and *sox4* morphant optic vesicle and retina from 18 to 72 hpf. 10-20 individuals were

analyzed for each time point (Student's *t*-test, P=0.017). (M-V) Representative transverse sections of control and *sox4* morphant retinas labeled for TUNEL-positive cells from 18 to 72 hpf. (W) Quantification of TUNEL-positive cells in control and *sox4* morphant optic stalk at 18 hpf. Arrows in N indicate increased TUNEL-positive cells in the optic stalk of an 18 hpf *sox4* morphant. All scale bars equal 50 μm.

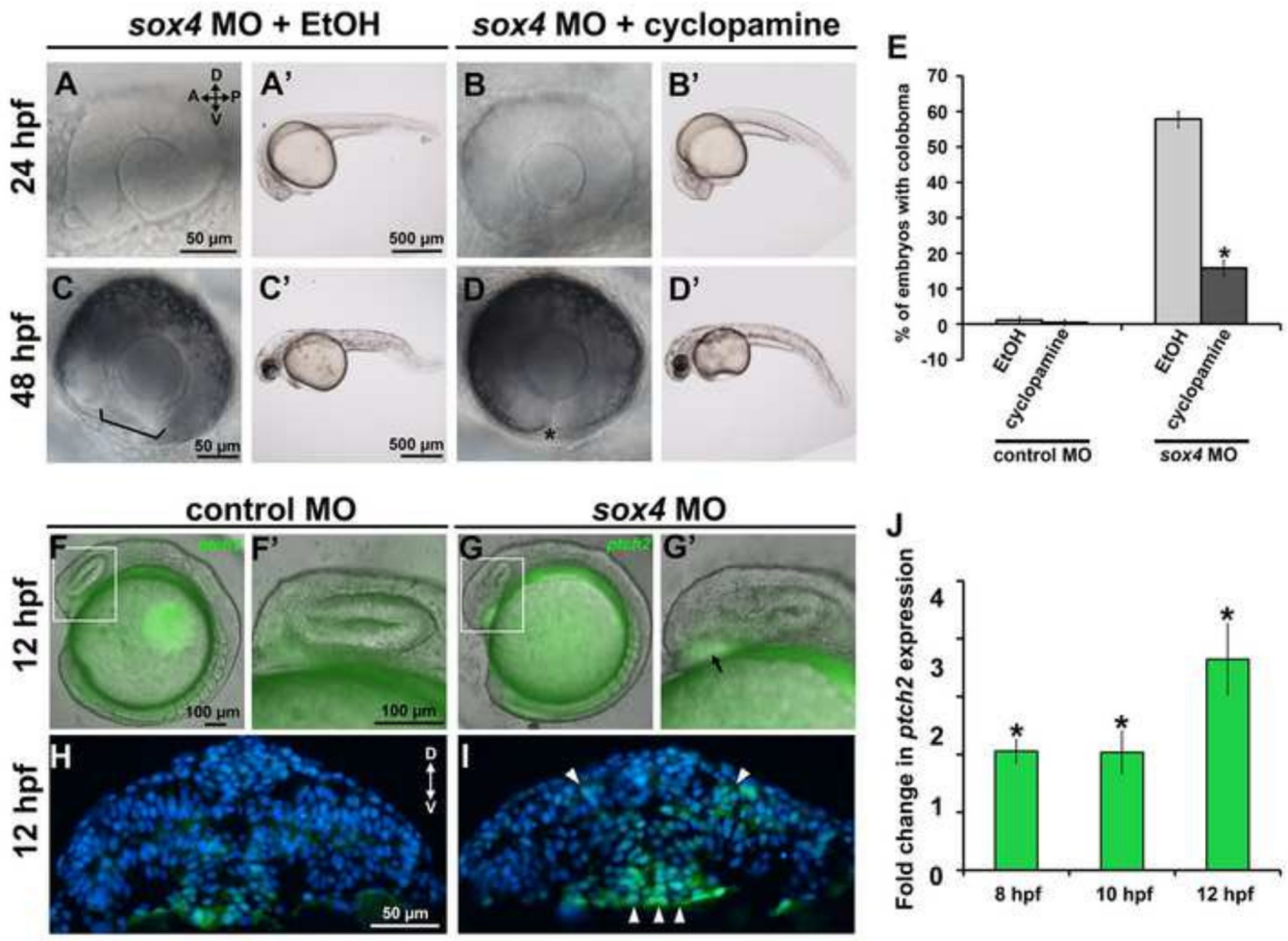

Figure 5. Hh signaling is elevated in Sox4-deficent zebrafish

(A-D') Representative eye and whole body images of vehicle-treated and cyclopamine-treated *sox4* morphants at 24 and 48 hpf. (E) Quantification of the percentage of coloboma in vehicle- and cyclopamine-treated control and *sox4* morphants (control morphants + vehicle: 1.14± 0.96% coloboma, n= 2/175; control morphants + cyclopamine: 0.49± 0.79% coloboma, n= 1/205; *sox4* morphants + vehicle: 57.78± 2.28% coloboma, n= 104/180; *sox4* morphants + cyclopamine: 15.87± 2.20% coloboma, n= 26/165; Fisher's exact test, $P<0.0001$). (F-I) Representative eye and body lateral images (F-G') and transverse sections (H, I) of *ptch2:EGFP*(+/−) transgenic embryos injected with control (F-F', H) or *sox4* MO (G-G', I) at 12 hpf. (J) qPCR analysis of *ptch2* expression in embryos injected with control or *sox4* MO at 8, 10, and 12 hpf. Relative transcript abundance was normalized to level of *atp5h* (three biological replicates; Student's *t*-test, $P<0.01$).

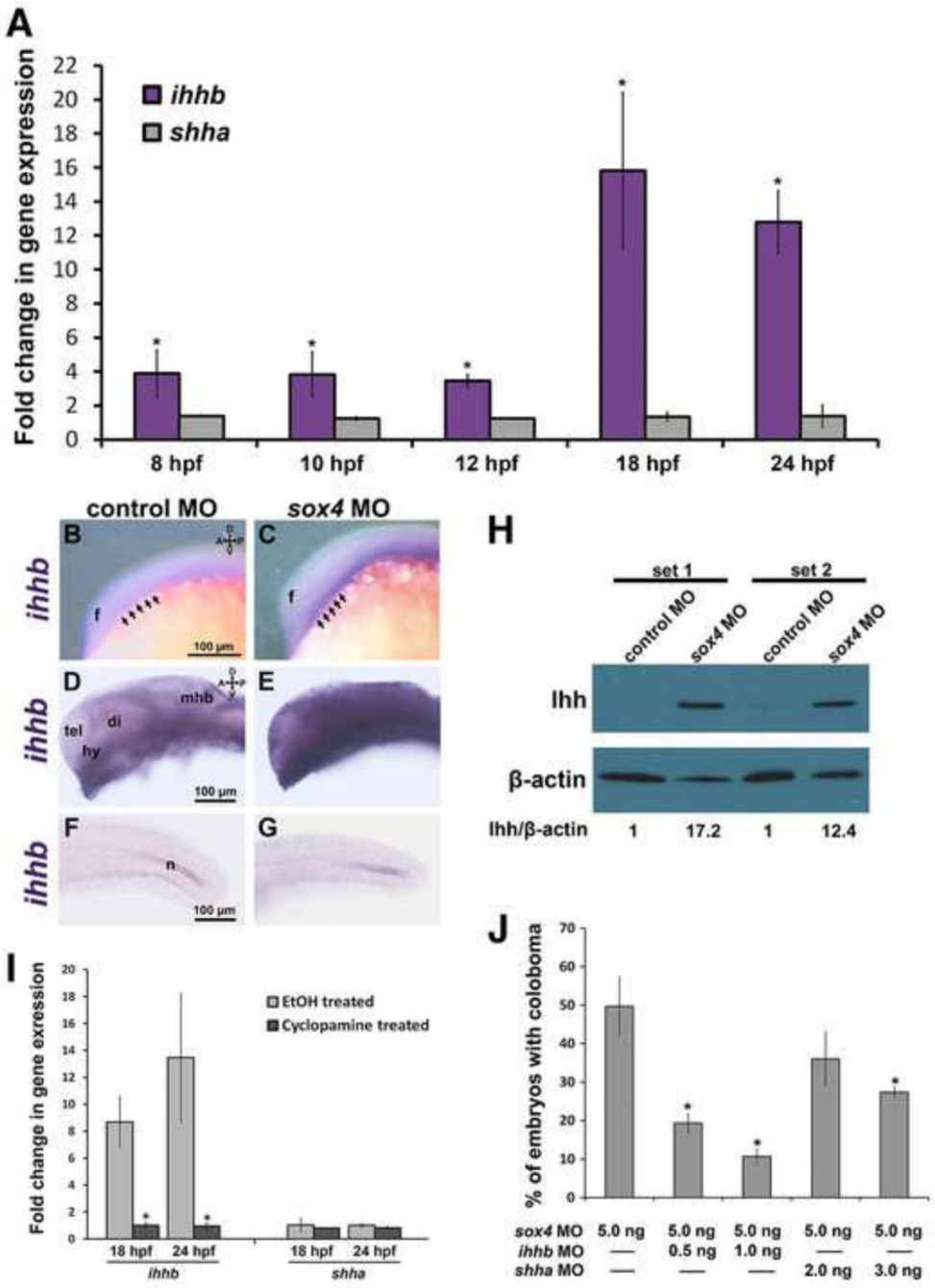

Figure 6. Sox4 negatively regulates *ihhb* expression

(A) *ihhb* and *shha* qPCR of mRNA from control and *sox4* morphant whole embryos at 8, 10 and 12 hpf, and heads at 18 and 24 hpf. Relative transcript abundance was normalized to level of *atp5h or gapdh*. Y axis represents the average ratio of normalized *sox4* morphant to control expression (three biological replicates; Student's *t*-test, P<0.01). (B-G) *Ihhb* expression in control and *sox4* morphants at 12 and 24 hpf detected by WISH. Representative images are presented from 15-20 individuals analyzed. Lateral images in B-E focus on the midline, therefore the eye is not visible. Arrows in B and C mark the ventral

forebrain at the level of the optic vesicle. (H) Western blot analysis of protein lysates from control or *sox4* morphant heads at 24 hpf. Two biological replicates were performed (sets 1 and 2) (I) qPCR of mRNA from vehicle- and cyclopamine-treated *sox4* morphants (Student's *t*-test, P<0.01). (J) Quantification of the proportion of embryos with coloboma at 48 hpf in *sox4* morphants co-injected with two different doses of either *ihhb* MO or *shha* MO (*sox4* MO alone: 51.24± 2.7%, n= 209/404; *sox4* MO + 0.5 ng/embryo *ihhb* MO: 19.33± 2.52%, n= 14/75; *sox4* MO + 1.0 ng/embryo *ihhb* MO: 10.67± 2.08%, n= 9/91; *sox4* MO + 2.0 ng/embryo of *shha* MO: 41.84± 5.62%, n= 53/125; *sox4* MO + 3.0 ng/embryo of *shha* MO, 34.39± 5.03%, n= 79/229) Fisher's exact test, P<0.0001 for *sox4* MO + *ihhb* MO; P= 0.1676 for *sox4* MO + 2.0 ng/embryo of *shha* MO; P=0.0001 for *sox4* MO + 3.0 ng/embryo of *shha* MO. f, forebrain; tel, telencephalon; di, diencephalon, hy, hypothalamus; mhb, midbrain-hindbrain boundary; n, notochord.

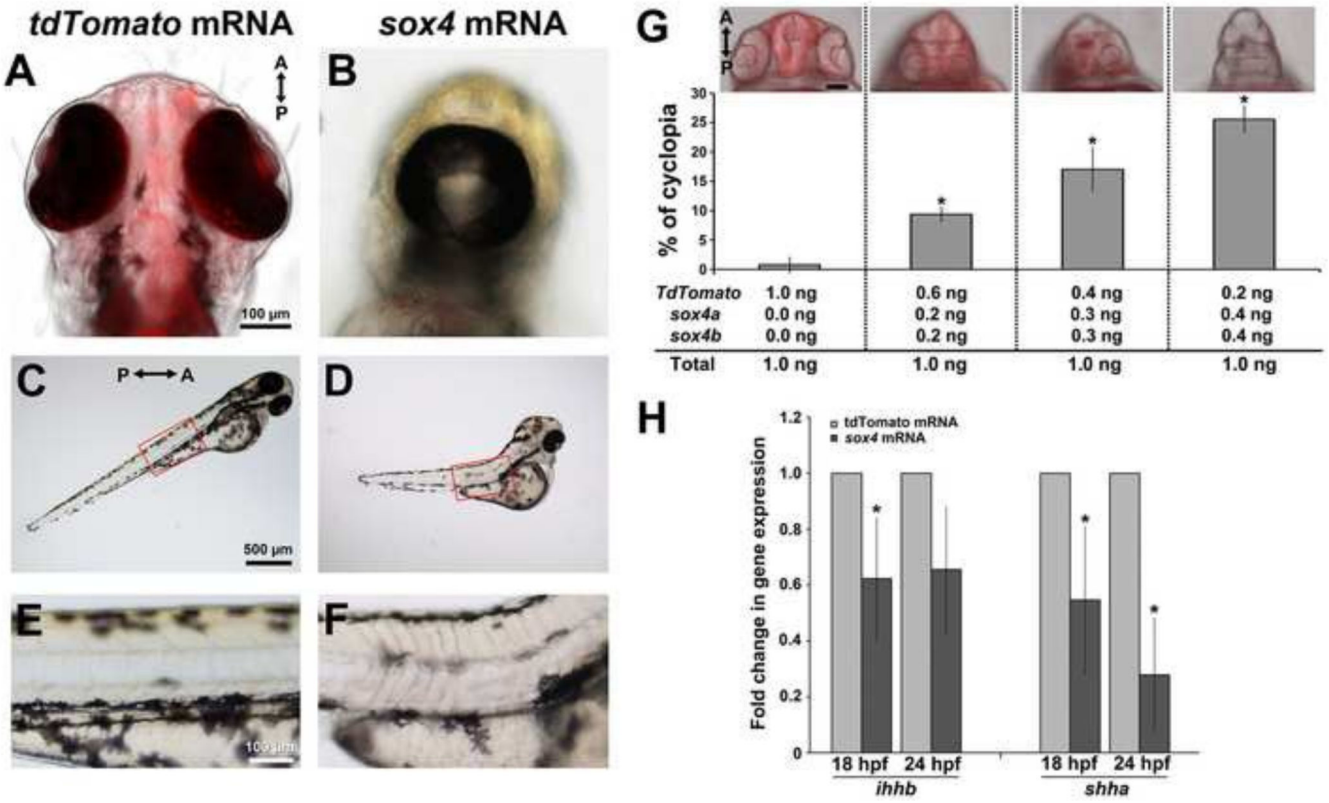

Figure 7. Overexpression of *sox4* inhibits Hh ligand expression and causes cyclopia

(A-F) Representative images of embryos injected with control *tdTomato* or *sox4* mRNA. (A-B) Representative images of the head were taken at 72 hpf from the ventral side. (C-F) Lateral views of body showing the somites. Insets in (C) and (D) were enlarged in (E) and (F). (G) Quantification of the percentage of cyclopia in embryos injected with different combinations of control and *sox4* mRNA. 1.0 ng/embryo *Td-tomato*: 0.76± 1.31%, n= 1/108; 0.2 ng *sox4a/b* + 0.6 ng *Td-tomato*/embryo: 9.35± 1.17%, n= 13/139; 0.3 ng *sox4a/b* + 0.4 ng *Td-tomato*/embryo: 17.03± 3.69%, n= 11/67; 0.4 ng *sox4a/b* + 0.2 ng *Td-tomato*/embryo: 25.56± 2.20%, n= 25/97. (H) qPCR analysis of *ihhb* and *shha* expression in control and *sox4* overexpressing heads at 18 and 24 hpf. In *sox4* mRNA injected embryos, *ihhb* expression was significantly decreased by 1.61-fold at 18 hpf (Student's *t*-test, $P<0.05$) and 1.51-fold at 24 hpf (Student's *t*-test, $P=0.057$). *Shha* expression was also significantly reduced following *sox4* mRNA injection at both 18 and 24 hpf (by 1.82-fold and 3.57-fold, respectively; Student's *t*-test, $P<0.05$).

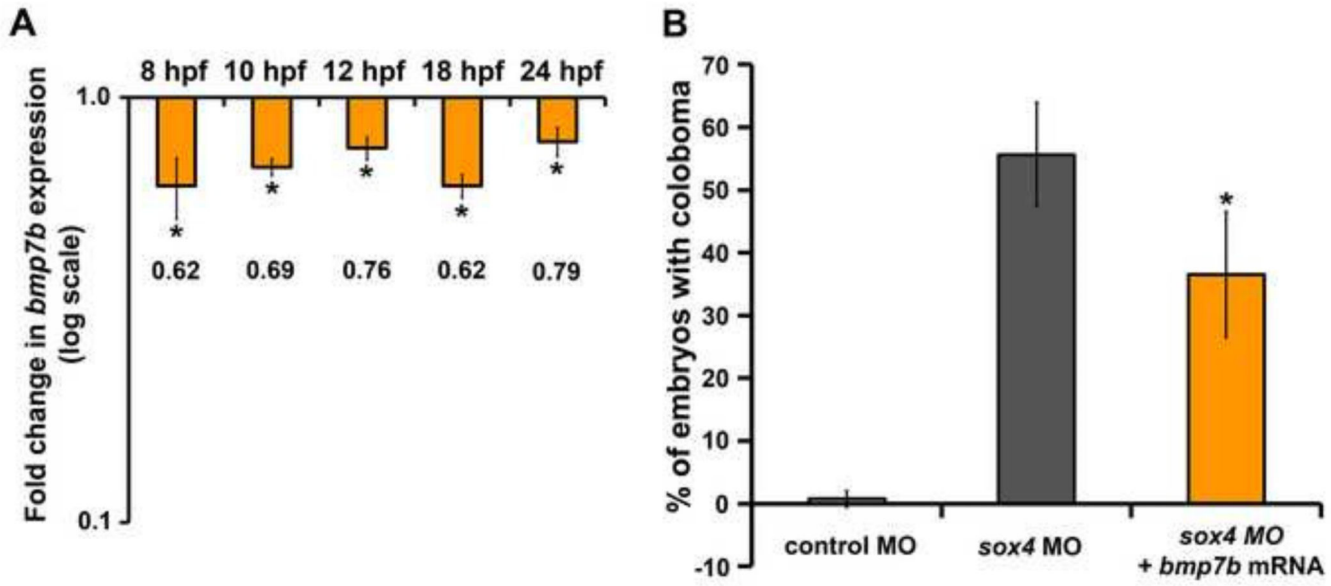

Figure 8. *Bmp7b* expression is reduced in *sox4* morphants

(A) qPCR analysis revealed a significant reduction in *bmp7b* expression in *sox4* morphant embryos at 8, 10, 12 hpf and heads at 18 and 24 hpf (Student's *t*-test, P<0.01). (B) *bmp7b* mRNA injection significantly reduced the proportion of embryos with coloboma in *sox4* morphants. Control MO only: 0.74± 1.28%, n= 1/110; *sox4* MO only: 55.66± 8.32%, n= 59/106; *sox4* MO+ *bmp7b* mRNA: 35.56± 10.02%, n= 29/80 (Student's t-test, P< 0.05).

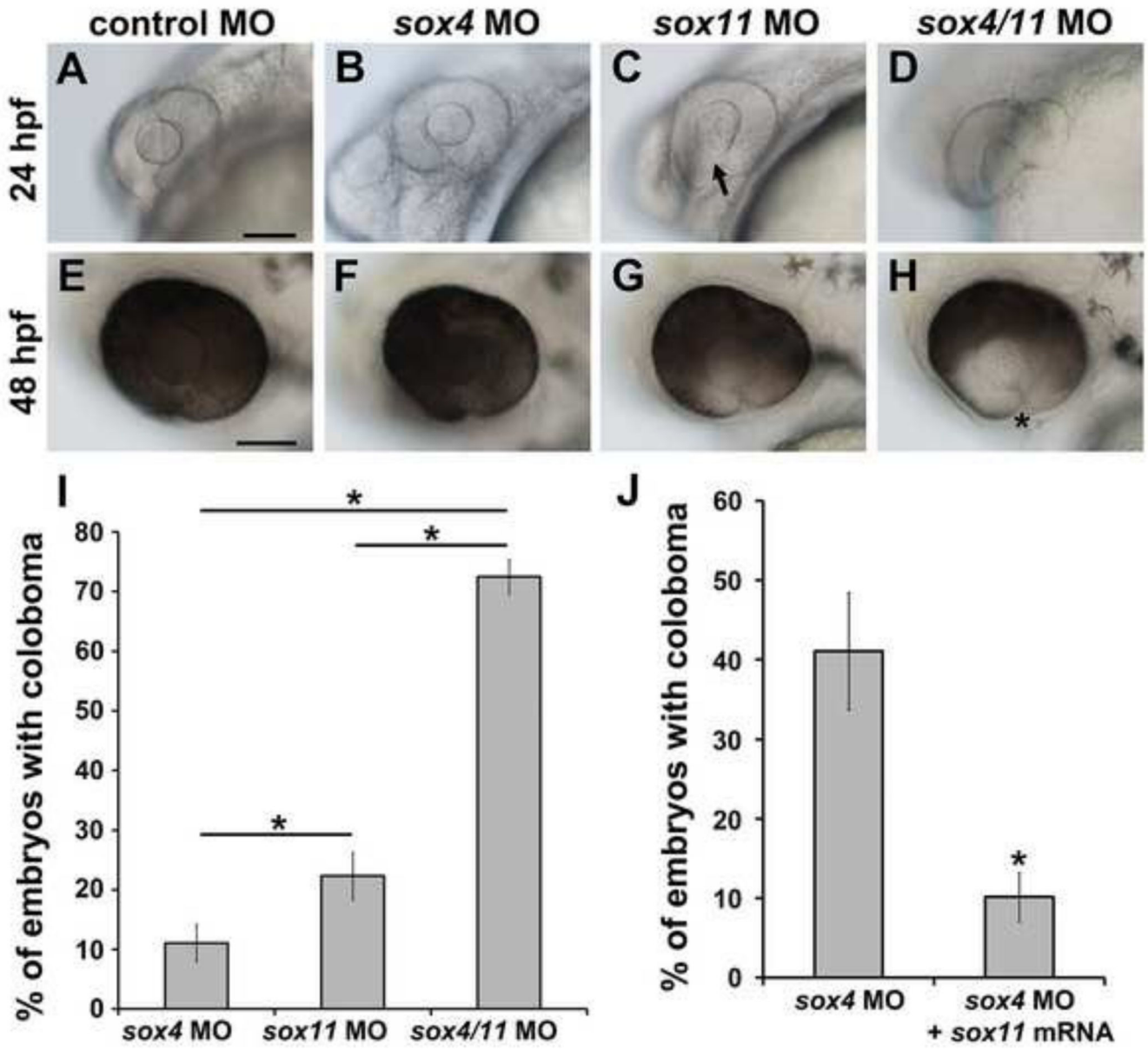

Figure 9. Synergistic effect of *sox4* and *sox11* knockdown on coloboma.

(A-H) Representative images of embryos injected with control MO (A, E), a half-dose of *sox4* MO (B, F), a half-dose of *sox11* MO (C, G), and half-doses of *sox4* and *sox11* MOs (D, H). (A, E) Half the normal dose of *sox4* MO caused a low incidence of mild coloboma. (C, G) Half the normal dose of *sox11* MO resulted in low incidence of coloboma and lens malformations at 24 hpf (C, arrow). (D, H) Injection of a half-dose of both *sox4* and *sox11* MO significantly increased the incidence of coloboma, and the coloboma phenotype was more severe compared to *sox4* or *sox11* morphants alone. (I) Quantification of the proportion of embryos with coloboma at 48 hpf (half-dose *sox4* MO, 11.05± 3.15%, n= 16/145; half-dose *sox11* MO, 22.31± 4.0%, n= 16/71; half-dose of both *sox4* and *sox11* MO, 72.47± 2.95%, n= 51/70; Fisher's exact test, P=0.0001). (J) Sox11 can compensate for the loss of Sox4. Injection of *sox11* mRNA into *sox4* morphants significantly reduced the

incidence of coloboma from 41.09±7.36% (n= 113/275) to 10.14± 3.09% (n= 28/276; Fisher's exact test, P<0.0001). All scale bars equal 100 μm.